Inorganic Chemistry

Article

pubs.acs.org/IC

Germyl- and Germylene-Bridged Complexes of Rh/Ir and Subsequent Chemistry of a Bridging Germylene Group

Md Hosnay Mobarok,[†] Robert McDonald,[†,‡] Michael J. Ferguson,[†,‡] and Martin Cowie*,[†]

[†]Department of Chemistry and [‡]X-ray Crystallography Laboratory, University of Alberta, Edmonton, Alberta, Canada, T6G 2G2

Supporting Information

ABSTRACT: A series of neutral and cationic germylene-bridged complexes and a neutral germyl(germylene) complex have been synthesized and characterized by NMR spectroscopy and X-ray crystallography. Reaction of 1 equiv of primary germanes, $RGeH_3$ (R = Ph, ^{t}Bu), with $[RhIr(CO)_3(dppm)_2]$ (**1**) at low-temperature yields $[RhIr(GeH_2R)(H)(CO)_3(dppm)_2]$ (R = Ph (**3**) or ^{t}Bu (**4**)), the products of single Ge−H bond activation, which upon warming transform to the germylene-bridged dihydrides, $[RhIr(H)_2(CO)_2(\mu\text{-GeHR})(dppm)_2]$ (R = Ph (**5**) or ^{t}Bu (**6**)) by activation of a second Ge−H bond accompanied by CO loss. Both classes of compounds have the diphosphines folded back in a "cradle-shaped" geometry. Although compound **5** reacts with additional phenylgermane at −40 °C to give a germylene-bridged/germyl product, $[RhIr(GeH_2Ph)(H)_2(CO)_2(\kappa^1\text{-dppm})(\mu\text{-GeHPh})(\mu\text{-H})(dppm)]$ (**7**), warming results in decomposition. However, reaction of **5** with 1 equiv of diphenylgermane at ambient temperature results in a novel mixed bis(μ-germylene) complex, $[RhIr(CO)_2(\mu\text{-GeHPh})(\mu\text{-GePh}_2)(dppm)_2]$ (**8**), containing both mono- and disubstituted germylene fragments. Reaction of 1 equiv of diphenylgermane with complex **1** produces a similar monogermylene-bridged product, $[RhIr(H)_2(CO)_2(\mu\text{-GePh}_2)(dppm)_2]$ (**9**), while reaction of **1** with 2 equiv of diphenylgermane yields the germyl/germylene product $[RhIr(H)(GeHPh_2)(CO)_3(\kappa^1\text{-dppm})(\mu\text{-GePh}_2)(dppm)]$ (**10**). The above reactions, incorporating first one and then a second equivalent of primary and secondary germanes, were studied by low-temperature multinuclear NMR spectroscopy, revealing details about the stepwise activations of multiple Ge−H bonds. Reaction of diphenylgermane with the cationic complex $[RhIr(CH_3)(CO)_2(dppm)_2][CF_3SO_3]$ (**2**) leads to a cationic A-frame-type germylene- and hydride-bridged product, $[RhIr(CO)_2(\mu\text{-H})(\mu\text{-GePh}_2)(dppm)_2][CF_3SO_3]$ (**3**), which reversibly activates H_2, yielding a germyl-bridged dihydride and reacts stoichiometrically with water, methanol, and HCl to yield the respective germanol, germamethoxy, and germylchloride products.

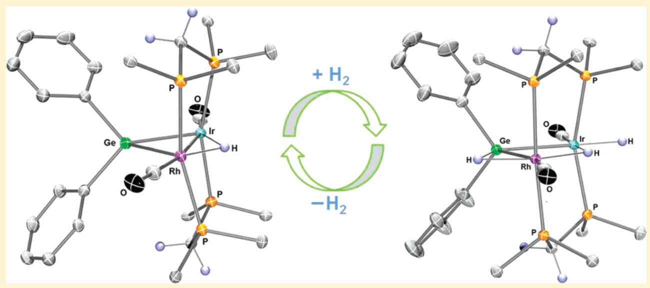

■ INTRODUCTION

There has been significant recent interest in the chemistry of transition-metal complexes containing germanium, in large part owing to the expanding role of this metal in transition-metal-catalyzed reactions.[1,2] For example, germanium has been shown to function as a modifier in the Pd- and Rh-mediated hydrogenation of citral and other unsaturated hydrocarbons[3] and can also give rise to improved selectivity in Ir/Pt-mediated hydrocracking.[4] However, little is understood about the roles of germanium in these processes or indeed about the potential roles that germanium may play in organotransition-metal chemistry in general. Some recent investigations have focused on the synthesis of germanium-containing polynuclear complexes as models for the above-noted heterogeneous catalysts,[5] although the reactivities of these model systems with H_2 have not yet been reported. Transition-metal complexes containing a terminal germylene group have also demonstrated interesting insertion reactions with small molecules such as CO_2,[6] nitrosobenzene,[7] and oxygen,[8] not unlike 2 + 2 cycloaddition reactions involving metal carbenes, and monometallic germyl complexes have given rise to Ge−Ge bond formation,[9] a necessary step in the generation of Ge-containing oligomers.

In contrast to the relatively underdeveloped chemistry of germanium, the neighboring congener Si has well-established chemistry with transition metals, in which silyl-[10] and silylene-containing complexes[11] have been shown to be involved in a range of homogeneously catalyzed processes such as olefin and ketone hydrosilylation,[12] dehydrogenative polymerization of silanes,[13] and silane alcoholysis.[14] On the basis of the close similarity of these two congeners, it can be anticipated that Ge should display related reactivity. Nevertheless, owing to their subtle differences, one can imagine that studies on one of these congeners can yield valuable information about the other, through the observation of species with one element that can model unobserved intermediates in the chemistry of the other, leading to a more complete understanding of both. For example, Tanabe et al. reported the stepwise generation of a $(GePh_2)_4$-containing metallacycle which served as a model for unobserved, early steps in silylene oligomerization.[9]

In a recent paper we reported a study in which activation of Si−H bonds in a series of primary and secondary silanes by

Received: September 30, 2011
Published: March 23, 2012

ACS Publications © 2012 American Chemical Society

heterobinuclear, dppm-bridged (dppm = $Ph_2PCH_2PPh_2$) complexes of Rh/Ir yielded silyl- and silylene-containing products.[15] Investigations of Si−H bond activation by closely related Rh_2[16] and Ir_2[17] complexes have also been reported. In the current study we continue our investigation of the Rh/Ir system to include the reactivity with germanes as a comparison with the related silane chemistry and to develop some of the chemistry of bridging-germylene groups. The Rh/Ir combination of metals exploits the strong tendency for low-valent Ir to undergo oxidative addition and the greater resulting bond strengths involving this metal, combined with the greater lability at Rh. This combination also takes advantage of the useful NMR characteristics of Rh as an aid in characterization of labile intermediates, which we anticipate will assist in determining the roles of the different metals in the stepwise activation of Ge−H bonds.

■ EXPERIMENTAL SECTION

General Comments. All solvents were dried (using appropriate drying agents), distilled before use, and stored under dinitrogen. Reactions were performed under an argon atmosphere using standard Schlenk techniques. $^tBuGeH_3$ was purchased from Gelest Inc., while Ph_2GeH_2 and $PhGeH_3$ were prepared by reaction of the corresponding chlorides (which were purchased from Alfa Inorganics and Gelest Inc., respectively) with $LiAlH_4$. $PhGeD_3$ was prepared analogously using $LiAlD_4$. Germanes were dried and distilled over CaH_2 under Ar and kept under subdued light. ^{13}C-enriched CO (99.4%) was purchased from Cambridge Isotope Laboratories, while ^{13}C-enriched methyl-triflate was purchased from Sigma-Aldrich. Compounds [RhIr(CO)$_3$(dppm)$_2$] (**1**)[18] and [RhIr(CH$_3$)(CO)$_2$(dppm)$_2$][CF$_3$SO$_3$] (**2**)[19] were prepared as previously reported. The tetraphenylborate and tetrakis(3,5-bis(trifluoromethyl)-phenyl)borate ($BAr^F{}_4{}^-$) salts of compound **2** (**2**[**BPh$_4$**] and **2**[**BAr$^F_4$**]) were synthesized by an anion exchange reaction of **2** using $NaBPh_4$ and $NaBAr^F{}_4$, respectively, in THF (1:1 stoichiometry; 30 min reaction time) followed by evaporation of THF and extraction of the synthesized complex with dichloromethane. NMR spectra were recorded on Varian Inova-400 or Varian Unity-500 spectrometers operating at the resonance frequencies of the NMR-active nuclei, given in the spectral information that follows. ^1H and $^{13}C\{^1H\}$ spectra were referenced internally to residual solvent proton signals relative to tetramethylsilane, whereas $^{31}P\{^1H\}$ and ^{19}F NMR spectra were referenced relative to external standards, 85% H_3PO_4 and CCl_3F, respectively. In the ^1H NMR spectral results the aromatic protons in the range δ 8.50−6.20 are not reported. The yields of all nonisolable complexes were determined by integration of their resonances in the ^{31}P NMR spectra, taking all resonances present as 100%. All spectra were recorded at 27 °C unless otherwise noted. Elemental analyses were performed by the Microanalytical Laboratory in the department.

Preparation of Compounds. *a. [RhIr(H)(GeH$_2$Ph)(CO)$_2$(μ-CO)(dppm)$_2$] (**3**).* In a septum-sealed NMR tube under an Ar atmosphere, [RhIr(CO)$_3$(dppm)$_2$] (**1**) (30 mg, 0.026 mmol) was dissolved in 0.7 mL of CD_2Cl_2 at ambient temperature, producing a dark orange solution, and then cooled to −78 °C. Addition of $PhGeH_3$ (3.2 μL, 0.026 mmol) by a microliter syringe resulted in a lightening of the solution color. Compound **3** was formed quantitatively after 30 min as confirmed by $^{31}P\{^1H\}$ NMR spectroscopy. No attempt was made to isolate this compound at this temperature. Further warming resulted in a subsequent transformation as described below. $^{31}P\{^1H\}$ NMR (−80 °C; CD_2Cl_2, 161.9 MHz): δ 37.5 (Rh−P, ddd, 1P, $^2J_{PP}$ = 240 Hz, $^1J_{RhP}$ = 133 Hz, $^2J_{PP}$ = 28 Hz), 28.8 (Rh−P, ddd, 1P, $^2J_{PP}$ = 142 Hz, $^1J_{RhP}$ = 126 Hz, $^2J_{PP}$ = 28 Hz), −5.5 (Ir−P, dd, 1P, $^2J_{PP}$ = 240 Hz, $^2J_{PP}$ = 18 Hz), −12.4 (Ir−P, dd, 1P, $^2J_{PP}$ = 142 Hz, $^2J_{PP}$ = 18 Hz), ^1H NMR (−80 °C; CD_2Cl_2, 399.8 MHz): δ 4.60 (CH_2, m, 1H), 4.23 (Ge−H, m, 1H), 4.14 (CH_2, m, 1H), 3.93 (CH_2, m, 1H), 3.87 (Ge−H, m, 1H), 2.59 (CH_2, m, 1H), −11.50 (Ir−H, ddd, 1H, $^2J_{trans\text{-}PH}$ = 125.0 Hz, $^4J_{distal(trans)\text{-}PH}$ = 27.0 Hz, $^2J_{cis\text{-}PH}$ = 13.0 Hz). $^{13}C\{^1H\}$ NMR (−80 °C; CD_2Cl_2, 100.5 MHz): δ 229.9 (μ-CO, dm, 1C, $^2J_{RhC}$ = 34 Hz), 198.2 (Rh−CO, dm, 1C, $^1J_{RhC}$ = 78 Hz), 178.0 (Ir−CO, bt, 1C, $^2J_{PC}$ = 12 Hz).

*b. [RhIr(H)(GeH$_2{}^t$Bu)(CO)$_2$(μ-CO)(dppm)$_2$] (**4**).* In a septum-sealed NMR tube under an Ar atmosphere, [RhIr(CO)$_3$(dppm)$_2$] (**1**) (32 mg, 0.028 mmol) was dissolved in 0.7 mL of CD_2Cl_2 at ambient temperature, producing a dark orange solution, and then cooled to −78 °C. A 3.8 μL (0.028 mmol) amount of $^tBuGeH_3$ was then added via a microliter syringe. No immediate color change was observed at this temperature; however, warming to −40 °C initiated a reaction, and after 30 min at this temperature complex **4** was formed in approximately 40% yield along with 60% of complex **1**. Again, no attempt was made to isolate this compound at this temperature. Further warming resulted in a subsequent transformation as described below. $^{31}P\{^1H\}$ NMR (−40 °C; CD_2Cl_2, 161.9 MHz): δ 39.4 (Rh−P, ddd, 1P, $^2J_{PP}$ = 245 Hz, $^1J_{RhP}$ = 107.5 Hz, $^2J_{PP}$ = 28 Hz), 29.8 (Rh−P, ddd, 1P, $^2J_{PP}$ = 152 Hz, $^1J_{RhP}$ = 96 Hz, $^2J_{PP}$ = 28 Hz), −5.5 (Ir−P, dd, 1P, $^2J_{PP}$ = 245 Hz, $^2J_{PP}$ = 18 Hz), −12.4 (Ir−P, 1P, dd, $^2J_{PP}$ = 152 Hz, $^2J_{PP}$ = 18 Hz). ^1H NMR (−40 °C; CD_2Cl_2, 399.8 MHz): δ 4.83 (CH_2, m, 1H), 3.98 (CH_2, m, 1H), 3.40 (Ge−H, m, 1H), 3.32 (CH_2, m, 1H), 3.29 (Ge−H, m, 1H), 2.56 (CH_2, m, 1H), 1.22 (^{t}Bu, s, 9H), −11.39 (Ir−H, ddd, 1H, $^2J_{trans\text{-}PH}$ = 125.5 Hz, $^4J_{distal(trans)\text{-}PH}$ = 30.3 Hz, $^2J_{cis\text{-}PH}$ = 12.5 Hz). $^{13}C\{^1H\}$ NMR (−40 °C; CD_2Cl_2, 100.5 MHz): δ 229.8 (μ-CO, dm, 1C, $^2J_{RhC}$ = 33 Hz), 198.5 (Rh−CO, dm, 1C, $^1J_{RhC}$ = 77 Hz), 178.0 (Ir−CO, bt, 1C, $^2J_{PC}$ = 12 Hz).

*c. [RhIr(H)$_2$(CO)$_2$(μ-GeHPh)(dppm)$_2$] (**5**).* In a 100 mL Schlenk tube, under anhydrous conditions and an Ar atmosphere, compound **1** (70 mg, 0.061 mmol) was dissolved in 5 mL of CH_2Cl_2 and cooled to 0 °C in an ice−water bath. Phenylgermane (7.5 μL, 0.061 mmol) was then added to the solution by a microliter syringe, resulting in an immediate color change from dark orange to light yellow. The reaction was allowed to stir for 10 min, followed by reduction of the solvent volume at the same temperature to approximately 1 mL in vacuo. Subsequent slow addition of 5 mL of pentane gave a pale yellow powder. The solid was further washed twice with 10 mL of pentane to give analytically pure compound in 73% isolated yield (56.6 mg). Anal. Calcd for $C_{58}H_{52}IrO_2P_4RhGe\cdot C_6H_6$: C, 56.86; H, 4.29. Found: C, 56.97; H, 4.44. $^{31}P\{^1H\}$ NMR (27 °C; CD_2Cl_2, 161.9 MHz): δ 27.8 (bm), 16.3 (bm), −8.3 (bm), −13.9 (bm). ^1H NMR (27 °C; CD_2Cl_2, 399.8 MHz): δ 5.42 (CH_2, m, 2H), 3.25 (CH_2, m, 1H), 2.92 (CH_2, m, 1H), −10.45 (Rh−H, bm, 1H), −11.65 (Ir−H, bm, 1H). $^{31}P\{^1H\}$ NMR (−40 °C; CD_2Cl_2, 161.9 MHz): δ 27.1 (Rh−P, dm, 1P, $^1J_{RhP}$ = 98 Hz), 16.9 (Rh−P, dm, 1P, $^1J_{RhP}$ = 125 Hz), −10.0 (Ir−P, m, 1P), −14.0 (Ir−P, m, 1P). ^1H NMR (−40 °C; CD_2Cl_2, 399.8 MHz): δ 5.40 (CH_2, m, 2H), 3.24 (CH_2, m, 1H), 2.85 (CH_2, m, 1H), −10.30 (Rh−H, ddm, 1H, $^2J_{trans\text{-}PH}$ = 150.0 Hz, $^1J_{RhH}$ = 12.0 Hz), −11.78 (Ir−H, dm, 1H, $^2J_{trans\ PH}$ = 127.1 Hz). $^{13}C\{^1H\}$ NMR (−40 °C, CD_2Cl_2, 100.5 MHz): δ 193.8 (Rh−CO, dm, 1C, $^1J_{RhC}$ = 62.8 Hz), 180.3 (Ir−CO, s, 1C), 49.8 (CH_2, m, 1C), 43.7 (CH_2, m, 1C). IR (CH_2Cl_2): ν(CO) = 1964 (s), 1946 (s) cm^{-1}, ν(M−H) = 2091 (w, br) cm^{-1}. Compound **5** was also produced upon warming the solution of **3** to 0 °C. [RhIr(D)$_2$(CO)$_2$(μ-GeDPh)(dppm)$_2$] (**5-D$_3$**) was prepared as described for **5** by reaction if **1** with $PhGeD_3$. ^2H NMR (−80 °C, CH_2Cl_2, 61.4 MHz): δ 6.92 (Ge−D, s, 1D), −10.47 (Rh−D, bs, 1D), −11.86 (Ir−D, s, 1D).

*d. [RhIr(H)$_2$(CO)$_2$(μ-GeH^{t}Bu)(dppm)$_2$] (**6**).* In a 100 mL Schlenk tube, under anhydrous conditions and an Ar atmosphere, compound **1** (65 mg, 0.057 mmol) was dissolved in 5 mL of benzene at ambient temperature. *tert*-Butylgermane (9.0 μL, 0.065 mmol) was then added to the solution by syringe, resulting in an immediate color change from dark orange to light yellow. The reaction was allowed to stir for 30 min, followed by reduction of solvent volume to approximately 1 mL in vacuo. Subsequent slow addition of pentane gave a pale yellow powder in 92% isolated yield (65.3 mg). X-ray quality crystals were grown by slow diffusion of diethyl ether into the concentrated CH_2Cl_2 solution of **6**. Anal. Calcd for $C_{56}H_{58}GeIrO_2P_4Rh$: C, 53.61; H, 4.66. Found: C, 53.69; H, 4.70. $^{31}P\{^1H\}$ NMR (27 °C, CD_2Cl_2, 201.6 MHz): δ 28.4 (Rh−P, dm, 1P, $^1J_{RhP}$ = 112 Hz), 15.3 (Rh−P, dm, 1P, $^1J_{RhP}$ = 117 Hz), −8.3 (Ir−P, m, 1P), −14.6 (Ir−P, m, 1P). ^1H NMR (27 °C, $CDCl_2$, 498.1 MHz): δ 6.70 (Ge−H, bs, 1H), 5.45 (CH_2, m, 2H), 3.22 (CH_2, m, 1H), 2.91 (CH_2, m, 1H), 1.59 (^{t}Bu, m, 9H), −10.65 (Rh−H, ddm, 1H, $^2J_{trans\text{-}PH}$ = 149.9 Hz, $^1J_{RhH}$ = 12.0 Hz), −11.78 (Ir−H, dm, 1H, $^2J_{trans\text{-}PH}$ = 126.5 Hz). $^{13}C\{^1H\}$ NMR

(27 °C, CD_2Cl_2, 100.5 MHz): δ 195.2 (Rh−CO, dm, 1C, $^1J_{RhC}$ = 66.5 Hz), 181.3 (Ir−CO, s, 1C), 51.8 (CH_2, m, 1C), 45.6 (CH_2, m, 1C), 30.9 (^{t}Bu, s, 1C), 30.6 (^{t}Bu, s, 3C). IR (CH_2Cl_2): ν(CO) = 1944, 1896 (s) cm^{-1}, ν(Ge−H) = 2097 (w) cm^{-1}. Compound **6** was also produced upon warming solutions of **4** to ambient temperature.

*e. [RhIr(GeH$_2$Ph)(H)$_2$(CO)$_2$(κ^1-dppm)(μ-GePhH)(μ-H)(dppm)] (**7**).* In a septum-sealed NMR tube under an Ar atmosphere, [RhIr(H)$_2$(CO)$_2$(μ-GeHPh)(dppm)$_2$] (**5**) (30 mg 0.023 mmol) was dissolved in 0.7 mL of CD_2Cl_2 and then cooled to −78 °C. A 3.2 μL (1.1 equiv) amount of $PhGeH_3$ was added to the NMR tube via a microliter syringe. No reaction was observed by NMR at this temperature. Upon warming to −40 °C, the intermediate **7** was observed in the $^{31}P\{^1H\}$ NMR spectrum in approximately 30% yield after 1 h reaction time. Further warming to −20 °C led to several unidentified products. $^{31}P\{^1H\}$ NMR (−40 °C, CD_2Cl_2, 161.9 MHz): δ 21.8 (Rh−P, dm, 1P, $^1J_{RhP}$ = 102 Hz), −10.5 (Ir−P, m, 1P), −18.3 (Ir−P, m, 1P), −28.4 (Pendent-P, m, 1P). ^{1}H NMR (−40 °C; CD_2Cl_2, 399.8 MHz): δ 5.22 (CH_2, m, 1H), 4.92 (CH_2, m, 1H), 3.67 (Ge−H, m, 1H), 3.58 (Ge−H, m, 1H), 3.31 (CH_2, m, 1H), 2.56 (CH_2, m, 1H), −12.10 (Rh−H, ddm, 1H, $^2J_{trans\text{-}PH}$ = 159 Hz, $^1J_{RhH}$ = 12.0 Hz), −12.58 (μ-H, b, 1H, $^1J_{RhH}$ = 14.0 Hz), −12.75 (Ir−H, dm, 1H, $^2J_{trans\text{-}PH}$ = 129 Hz).

*f. [RhIr(CO)$_2$(μ-GeHPh)(μ-GePh$_2$)(dppm)$_2$] (**8**).* A 74 mg (0.058 mmol) amount of [RhIr(H)$_2$(CO)$_2$(μ-GeHPh)(dppm)$_2$] (**5**) in a Schlenk flask was dissolved in 10 mL of CH_2Cl_2 followed by addition of 11 μL (0.058 mmol) of Ph_2GeH_2. The reaction mixture was stirred gently for 24 h, during which time the yellow solution of **5** turned orange. The solvent volume was reduced to approximately 1 mL under high vacuum, and the solution was layered with 3 mL of pentane, yielding light yellow crystals (suitable for X-ray analysis) of compound **8** after 48 h in 77% yield. Anal. Calcd for $C_{70}H_{60}Ge_2IrO_2P_4Rh$: C, 56.17; H, 4.01. Found: C, 55.91; H, 4.16. $^{31}P\{^1H\}$ NMR (27 °C; CD_2Cl_2, 201.6 MHz): δ 35.8 (Rh−P, ddd, 1P, $^1J_{RhP}$ = 112 Hz, $^2J_{PP}$ = 116 Hz, $^2J_{PP}$ = 28 Hz), 24.4 (Rh−P, ddd, 1P, $^1J_{RhP}$ = 115 Hz, $^2J_{PP}$ = 140 Hz, $^2J_{PP}$ = 28 Hz), 7.8 (Ir−P, dd, 1P, $^2J_{PP}$ = 116 Hz, $^2J_{PP}$ = 20 Hz), −7.9 (Ir−P, dd, 1P, $^2J_{PP}$ = 140 Hz, $^2J_{PP}$ = 20 Hz). ^{1}H NMR (27 °C; CD_2Cl_2, 498.1 MHz): δ 6.14 (Ge−H, m, 1H), 5.13 (CH_2, m, 1H), 4.49 (CH_2, m, 1H), 3.02 (CH_2, m, 1H), 2.94 (CH_2, m, 1H). $^{13}C\{^1H\}$ (CD_2Cl_2, 100.5 MHz): δ 200.5 (Rh−CO, dm, 1C, $^1J_{RhC}$ = 76 Hz), 187.0 (Ir−CO, bs, 1C), 37.5 (CH_2, m, 1C), 34.1 (CH_2, m, 1C)

*g. [RhIr(H)$_2$(CO)$_2$(μ-GePh$_2$)(dppm)$_2$] (**9**).* Under an Ar atmosphere, 100 mg of compound **1** (0.087 mmol) in a Schlenk tube was dissolved in 20 mL of CH_2Cl_2. The solution was then cooled to 0 °C in an ice−water bath, 17.8 μL (1.1 equiv) of Ph_2GeH_2 was added by syringe to the vigorously stirred solution of **1**, and the reaction was left for 6 h at this temperature under a dynamic Ar flow (which is important for effective removal of released CO; otherwise, the reaction mainly gave a mixture of complexes **9** and **10**). During this time the color of the solution lightened. The solvent was reduced to 1 mL in vacuo, and the remaining solution was layered with 3 mL of pentane. Colorless crystals were separated after 24 h. Isolated yield 40% (47.0 mg). Anal. Calcd for $C_{64}H_{56}GeIrO_2P_4Rh$: C, 56.95; H, 4.15. Found: C, 56.72; H, 4.29. $^{31}P\{^1H\}$ NMR (27 °C; CD_2Cl_2, 161.9 MHz): δ 27.5 (Rh−P, m, 1P), 18.1 (Rh−P, m, 1P). −0.2 (Ir−P, m, 1P), −8.3 (Ir−P, m, 1P). ^{1}H NMR (27 °C; CD_2Cl_2, 399.8 MHz): δ 4.01 (CH_2, bm, 1H), 3.82 (CH_2, bm, 1H), 2.95 (CH_2, bm, 1H), 2.55 (CH_2, bm, 1H), −10.78 (bm), −11.09 (bm, 1H). $^{31}P\{^1H\}$ NMR (−80 °C; CD_2Cl_2, 161.9 MHz): δ 27.1(Rh−P, m, 1P), 17.8 (Rh−P, m, 1P), −0.8 (Ir−P, m, 1P), −8.6 (Ir−P, m, 1P). ^{1}H NMR (−80 °C; CD_2Cl_2, 399.8 MHz): δ 4.12 (CH_2, m, 1H), 3.95 (CH_2, m, 1H), 3.00 (CH_2, bm, 1H), 2.63 (CH_2, m, 1H), −10.76 (Rh−H, ddm, 1H, $^2J_{trans\text{-}PH}$ = 129.0 Hz, $^1J_{Rh-H}$ = 13.0 Hz), −11.09 (Ir−H, dm, 1H, $^2J_{trans\text{-}PH}$ = 115.0 Hz). $^{13}C\{^1H\}$ NMR (27 °C; CD_2Cl_2, 100.5 MHz): δ 197.9 (Rh−CO, dt, 1C, $^1J_{RhC}$ = 69 Hz, $^2J_{PC}$ = 10 Hz), 182.9 (Ir−CO, t, 1C, $^2J_{PC}$ = 13 Hz).

*h. [RhIr(H)(GePh$_2$H)(CO)$_3$(κ^1-dppm)(μ-GePh$_2$)(dppm)] (**10**).* In a Schlenk tube 100 mg (0.087 mmol) of compound **1** was dissolved in 5 mL of benzene at ambient temperature. Three freeze−pump−thaw cycles were applied to the solution, followed by addition of 64 μL (4 equiv) of Ph_2GeH_2. After stirring the solution overnight in the sealed Schlenk tube, the solvent volume was reduced in vacuo to 2 mL. Subsequent addition of 10 mL of pentane gave rise to a yellow powder. Orange crystals were obtained by diffusion of pentane into a concentrated fluorobenzene solution of the compound. Isolated yield 68% (95.0 mg). Anal. Calcd for $C_{77}H_{66}Ge_2IrO_3P_4Rh\cdot1.5C_6H_5F$: C, 59.05; H, 4.21. Found: C, 59.32; H, 4.41. $^{31}P\{^1H\}$ NMR (27 °C; C_6D_6, 161.9 MHz): δ 4.2 (Rh−P, ddd, 1P, $^1J_{RhP}$ =108 Hz, $^2J_{PP}$ = 108 Hz, $^3J_{PP}$ = 5 Hz), −2.3 (Ir−P, dd, 1P, $^2J_{PP}$ = 45 Hz, $^3J_{PP}$ = 5 Hz), −8.3 (Ir−P, ddd, 1P, $^2J_{PP}$ = 108 Hz, $^2J_{RhP}$ = 8 Hz, $^4J_{PP}$ = 8 Hz), −28.5 (pendent-P, dd, 1P, $^2J_{PP}$ = 45 Hz, $^4J_{PP}$ = 8 Hz). ^{1}H NMR (27 °C; C_6D_6, 498.1 MHz): δ 5.65 (Ge−H, d, 1H, $^3J_{PH}$ = 6.1 Hz), 5.16 (CH_2, m, 1H), 3.88 (CH_2, m, 1H), 3.54 (CH_2, m, 1H), 3.26 (CH_2, m, 1H), −10.82 (Ir−H, dd, 1H, $^2J_{PH}$ = 19.6 Hz, $^2J_{PH}$ = 14.6 Hz). $^{13}C\{^1H\}$ NMR (27 °C; CD_2Cl_2, 100.5 MHz): δ 202.4 (Rh−CO, dm, 1C, $^1J_{RhC}$ = 43.8 Hz), 200.5 (Rh−CO, dm, 1C, $^1J_{RhC}$ = 43.8 Hz), 184.8 (Ir−CO, bs, 1C), 58.3 (CH_2, m, 1C), 38.5 (CH_2, m, 1C).

*i. [RhIr(CH$_3$)(GeHPh$_2$)(CO)(μ-H)(μ-CO)(dppm)$_2$][CF$_3$SO$_3$] (**11**).* Under Ar, 30 mg (0.023 mmol) of [RhIr(CH_3)(CO)$_2$(dppm)$_2$]-[CF_3SO_3] (**2**) was taken into an NMR tube, dissolved in 0.7 mL of CD_2Cl_2, and cooled to −78 °C in an acetone−dry ice bath. A 4.3 μL (0.023 mmol) amount of diphenylgermane was added by a microliter syringe, and the reaction was monitored by low-temperature NMR spectroscopy. Immediately after addition of diphenylgermane the dark orange color of the solution lightened. Between −80 and −60 °C NMR analysis indicated quantitative formation of [RhIr(CH_3)-($GeHPh_2$)(CO)(μ-H)(μ-CO)(μ-dppm)$_2$][CF_3SO_3] (**11**) in solution. No attempt was made to isolate this compound at this temperature. ^{13}C-enriched compound **11** was prepared as discussed above by reacting ^{13}C-enriched [RhIr($^{13}CH_3$)(^{13}CO)$_2$(dppm)$_2$][CF_3SO_3] (**2**) with Ph_2GeH_2. $^{31}P\{^1H\}$ NMR (−80 °C; CD_2Cl_2, 161.9 MHz): δ 28.3 (Rh−P, dm, 2P, $^1J_{RhP}$ = 140 Hz), −9.1 (Ir−P, m, 2P). ^{1}H NMR (−80 °C; CD_2Cl_2, 399.8 MHz): δ 5.09 (Ge−H, t, 1H, $^3J_{PH}$ = 13.0 Hz), 4.10 (CH_2, m, 2H), 3.40 (CH_2, m, 2H), 0.49 (CH_3, t, 3H, $^3J_{PH}$ = 6.8 Hz), −8.94 (μ-H, dm, 1H, $^1J_{RhH}$ = 13.6 Hz). $^{13}C\{^1H\}$ (−80 °C; CD_2Cl_2, 100.5 MHz): δ 214.8 (μ-CO, dm, 1C, $^1J_{RhC}$ = 29 Hz), 173.3 (Ir−CO, t, 1C, $^2J_{PC}$ = 9.0 Hz), 32.7 (CH_2, m, 2C) 15.1 (CH_3, dt, 1C, $^1J_{RhC}$ = 28.0 Hz, $^2J_{PC}$ = 6.0 Hz). ^{19}F NMR (−80 °C; CD_2Cl_2, 376.3 MHz): δ 79.3 (CF_3SO_3, s, 3F).

*j. [RhIr(CH$_3$)(CO)$_2$(μ-GeHPh$_2$)(μ-H)(dppm)$_2$][CF$_3$SO$_3$] (**12**).* Method 1: Warming the solution of compound **11** to −20 °C resulted in a color change of the solution to light green from light orange. $^{31}P\{^1H\}$ NMR suggested quantitative formation of compound **12**. Method 2: 70 mg (0.055 mmol) of compound **2** in a Schlenk tube was dissolved in 3 mL of THF followed by three freeze−pump−thaw cycles. The reaction flask was then cooled to −15 °C in a salt−ice water bath. A 10.2 μL (0.055 mmol) amount of Ph_2GeH_2 was dissolved in another Schlenk tube, and the solution was cannula transferred to the first flask. The reaction was stirred for 30 min at this temperature, during which time a greenish-yellow precipitate settled at the bottom of the flask. After removal of THF via cannula, the solids were washed with ether to give analytically pure complex. Isolated yield 67% (55.2 mg). The complex was stable at ambient temperature in the solid state under an inert atmosphere; however, it was unstable above 20 °C in a solution of CH_2Cl_2. Anal. Calcd for $C_{66}H_{59}F_3IrO_5P_4RhGeS$: C, 52.42; H, 3.91. Found: C, 52.79; H, 4.23. ^{13}C-enriched compound **12** was prepared under similar conditions as mentioned above by reacting [RhIr($^{13}CH_3$)(^{13}CO)$_2$(dppm)$_2$][CF_3SO_3] (**2**) with Ph_2GeH_2. $^{31}P\{^1H\}$ NMR (−20 °C; CD_2Cl_2, 161.9 MHz): δ 21.4 (Rh−P, dm, 2P, $^1J_{RhP}$ = 99 Hz), −15.6 (Ir−P, m, 2P). ^{1}H NMR (−20 °C; CD_2Cl_2, 399.8 MHz): δ 4.08 (CH_2, m, 2H), 3.36 (CH_2, m, 2H), 0.89 (CH_3, t, 3H, $^3J_{PH}$ = 6.4 Hz), −1.92 (μ-Ge−H, ddm, 1H, $^1J_{RhH}$ = 25.2 Hz, $^2J_{HH}$ = 7.0 Hz), −9.23 (ddm, μ-H, 1H, $^1J_{RhH}$ = 16.8 Hz, $^2J_{HH}$ = 7.0 Hz). $^{13}C\{^1H\}$ NMR (−20 °C, CD_2Cl_2, 100.5 MHz): δ 192.4 (Rh−CO, dt, 1C, $^1J_{RhC}$ = 78.5 Hz, $^2J_{PC}$ = 14.2 Hz), 177.5 (Ir−CO, t, 1C, $^2J_{PC}$ = 7.8 Hz), 36.9 (CH_2, m, 2C), −25.1 (CH_3, bt, 1C, $^2J_{PC}$ = 7.0 Hz). ^{19}F NMR (−20 °C; CD_2Cl_2, 376.3 MHz): δ 79.3 (CF_3SO_3, s, 3F).

*k. [RhIr(CO)$_2$(μ-H)(μ-GePh$_2$)(dppm)$_2$][CF$_3$SO$_3$] (**13**).* Method 1: As the solution of compound **12** was warmed to ambient temperature the color turned dark green from light green within a period of 2 h. $^{31}P\{^1H\}$ NMR suggested quantitative formation of compound **13**. Method 2: 70 mg (0.055 mmol) of compound **2** in a Schlenk tube was dissolved in 3 mL of dry CH_2Cl_2 followed by three freeze−pump−

thaw cycles. A 10.2 μL (0.055 mmol) amount of Ph_2GeH_2 was dissolved in the same solvent in another Schlenk tube, and the solution was cannula transferred to the former flask at ambient temperature. The reaction was left stirring gently for 4 h, during which time the dark orange reaction mixture turned to light yellow then to dark green. Addition of 10 mL of pentane resulted in a bright green powder in 90% isolated yield (73.3 mg). Anal. Calcd for $C_{65}H_{55}F_3IrO_5P_4RhGeS$: C, 51.97; H, 3.78. Found: C, 52.16; H, 3.70. The same complexes having $[BPh_4]^-$ and $[BAr^F_4]^-$ anions (**13**$[\mathbf{BPh_4}]$ and **13**$[\mathbf{BAr^F_4}]$) were synthesized by the following procedure: Under an atmosphere of Ar, 53 mg (0.036 mmol) of **2**$[\mathbf{BPh_4}]$ or 72 mg of **2**$[\mathbf{BAr^F_4}]$ (0.036 mmol) was dissolved in 1 mL of THF or diethyl ether, respectively, in a 10 mL Schlenk tube, followed by addition of 6.8 μL (0.036 mmol) of Ph_2GeH_2 by a microliter syringe at ambient temperature. After 4 h the dark green solution was layered with pentane in both cases. Dark-yellow crystals (suitable for X-ray analysis) of both compounds were separated after 24 h in 80% (48.5 mg) and 83% (64 mg) isolated yield, respectively. ^{13}C-enriched compound **13** was prepared as noted above by reacting ^{13}C-enriched $[RhIr(^{13}CH_3)(^{13}CO)_2(dppm)_2][CF_3SO_3]$ (**2**) with Ph_2GeH_2. $^{31}P\{^1H\}$ NMR (27 °C; CD_2Cl_2, 201.6 MHz): δ 24.3 (Rh−P, dm, 2P, $^1J_{RhP}$ = 100 Hz), 0.5 (Ir−P, m, 2P). ^{1}H NMR (27 °C; CD_2Cl_2, 498.1 MHz): δ 4.83 (CH_2, m, 2H), 3.69 (CH_2, m, 2H), −9.91 (dm, μ-H, 1H, $^1J_{RhH}$ = 18.9 Hz). $^{13}C\{^1H\}$ NMR (27 °C, CD_2Cl_2, 125.7 MHz): 196.4 (Rh−CO, dt, 1C, $^1J_{RhC}$ = 67.9 Hz, $^2J_{PC}$ = 14.0 Hz), 185.5 (Ir−CO, t, 1C, $^2J_{PC}$ = 8.0 Hz), 37.9 (CH_2, m, 2C). ^{19}F NMR (27 °C; CD_2Cl_2, 376.3 MHz): δ 79.1 (CF_3SO_3, s, 3F).

*l. $[RhIr(H)(CO)_2(\mu\text{-}GeHPh_2)(\mu\text{-}H)(dppm)_2][CF_3SO_3]$ (**14**).* Method 1: Under an Ar atmosphere 50 mg of $[RhIr(CO)_2(\mu\text{-}H)(\mu\text{-}GePh_2)(dppm)_2][CF_3SO_3]$ (**13**) (0.033 mmol) was dissolved in a septum-sealed Schlenk tube with 1 mL of CH_2Cl_2. A 6.1 μL (0.033 mmol) amount of Ph_2GeH_2 was then introduced to the solution via microliter syringe. The dark green solution turned orange within 3 h. Addition of 2 mL of pentane gave rise to a pale yellow powder in 76% isolated yield (38 mg). Method 2: A septum-sealed NMR tube containing 50 mg (0.033 mmol) of $[RhIr(CO)_2(\mu\text{-}H)(\mu\text{-}GePh_2)(dppm)_2][CF_3SO_3]$ (**13**) in 0.7 mL of CD_2Cl_2 was pressurized with 1 atm of H_2. Within 5 min the dark green solution turned orange. Multinuclear NMR suggested quantitative conversion of **13** to **14**. Addition of 2 mL of pentane yielded a pale yellow powder as before in 85% isolated yield (42.5 mg). The deuterium isotopologue of **14**, $[RhIr(D)(CO)_2(\mu\text{-}GeDPh_2)(\mu\text{-}H)(dppm)_2][CF_3SO_3]$ (**14-D$_2$**), was synthesized by reaction of **13** with 1 atm pressure of D_2 under similar conditions. Method 3: To a septum-sealed NMR tube containing a solution of 50 mg (0.033 mmol) of compound **13** in 0.7 mL of CD_2Cl_2 was added 6.1 μL (0.033) of Ph_2SiH_2 via microliter syringe. The dark green solution slowly turned orange over a period of 6 h. Addition of 2 mL of pentane yielded a pale yellow powder. The same complex with $[BPh_4]^-$ and $[BAr^F_4]^-$ anions, **14**$[\mathbf{BPh_4}]$ and **14**$[\mathbf{BAr^F_4}]$, was synthesized by the following procedure: Under an atmosphere of Ar, 70 mg of **13**$[\mathbf{BPh_4}]$ or 90 mg of **13**$[\mathbf{BAr^F_4}]$ was dissolved in 1 mL of CH_2Cl_2 in a 10 mL Schlenk tube, followed by pressurization of the flask with 1 atm of H_2. Within 5 min the dark green solution turned orange in both cases, and no significant reaction rate difference was observed with these reactions compared to that of described in method 2 with OTf^- as the counteranion. The solvent in the solution of **14**$[\mathbf{BPh_4}]$ was removed under high vacuum, and the pale yellow solid was redissolved in 0.5 mL of THF. Layering with 1 mL of ether in an NMR tube gave rise to light-yellow X-ray quality crystals (suitable for X-ray analysis) of **14**$[\mathbf{BPh_4}]$ after 6 h in 75% isolated yield. Anal. Calcd for $C_{88}H_{77}BGeIrO_2P_4Rh$: C, 63.28; H, 4.61. Found: C, 63.49; H, 4.72. ^{13}C-enriched compound **14** was prepared as noted above by reacting ^{13}C-enriched $[RhIr(^{13}CH_3)(^{13}CO)_2(dppm)_2][CF_3SO_3]$ (**2**) with Ph_2GeH_2. $^{31}P\{^1H\}$ NMR (27 °C; CD_2Cl_2, 161.9 MHz): δ 22.9 (Rh−P, m, 1P), −11.5 (Ir−P, bm). ^{1}H NMR (27 °C; CD_2Cl_2, 498.1 MHz): δ 4.33 (CH_2, m, 2H), 3.47 (CH_2, bm, 2H), −2.00 (μ-Ge−H, b, 1H); −9.62 (Ir−H, b, 1H), −10.30 (μ-H, b, 1H). $^{31}P\{^1H\}$ NMR (−80 °C; CD_2Cl_2, 161.9 MHz): δ 22.5 (Rh−P, dm, 1P, $^1J_{RhP}$ = 102 Hz), −12.6 (Ir−P, m). ^{1}H NMR (−80 °C; CD_2Cl_2, 399.9 MHz): δ 4.15 (CH_2, m, 2H), 3.05 (CH_2, bm, 2H), −2.77 (μ-Ge−H, dm, 1H, $^1J_{RhH}$ = 27.6 Hz), −9.24 (Ir−H, s, 1H), −9.81 (μ-H, dm, 1H, $^1J_{RhH}$ = 18.8 Hz). $^{13}C\{^1H\}$ NMR (−40 °C; CD_2Cl_2, 125.7 MHz): δ 193.1 (Rh−CO, dt, 1C, $^1J_{RhC}$ = 80.7 Hz, $^2J_{PC}$ = 15.0 Hz), 185.5 (Ir−CO, s, 1C), 35.4 (CH_2, m, 2C). ^{19}F NMR (−80 °C; CD_2Cl_2, 376.3 MHz): δ 79.2 (CF_3SO_3, s, 3F).

*m. $[RhIr(CO)_2(Ge(OH)Ph_2)(\mu\text{-}H)_2(dppm)_2][CF_3SO_3]$ (**15**).* To a septum-sealed Schlenk tube containing 70 mg (0.047 mmol) of compound **13** in 2 mL of CH_2Cl_2 under argon was added 0.9 μL (0.050 mmol) of deoxygenated water. The dark green solution changed to orange within 5−10 min. After 30 min, addition of 5 mL of ether resulted in a dark orange solid in 83% isolated yield (58.9 mg). Anal. Calcd for $C_{65}H_{57}F_3GeIrO_6P_4RhS$: C, 51.55; H, 3.76. Found: C, 51.61; H, 3.83. X-ray quality crystals were obtained by layering diethyl ether over a concentrated CH_2Cl_2 solution of **15**. The deuterium isotopologue of **15**, $[RhIr(CO)_2(Ge(OD)Ph_2)(\mu\text{-}D)(\mu\text{-}H)(dppm)_2][CF_3SO_3]$ (**15-D$_2$**), was synthesized by reaction of **13** with 1 equiv of D_2O under similar conditions. $^{31}P\{^1H\}$ NMR (27 °C; CD_2Cl_2, 161.9 MHz): δ 24.4 (Rh−P, dm, 2P, $^1J_{RhP}$ = 105 Hz), −5.7 (Ir−P, m, 2P). ^{1}H NMR (27 °C; CD_2Cl_2, 498.1 MHz): δ 3.47 (CH_2, bm, 4H), 1.41 (O−H, b, 1H), −9.81 (μ-H, b, 1H), −12.05 (μ-H, b, 1H). $^{13}C\{^1H\}$ NMR (27 °C; CD_2Cl_2, 125.7 MHz): δ 186.2 (Rh−CO, dt, 1C, $^1J_{RhC}$ = 77.3 Hz, $^2J_{PC}$ = 17.0 Hz), 176.4 (Ir−CO, t, 1C, $^2J_{PC}$ = 11.6 Hz), 36.8 (CH_2, m, 2C). ^{19}F NMR (27 °C; CD_2Cl_2, 376.3 MHz): δ 79.1 (CF_3SO_3, s, 3F). $^2H\{^1H\}$ NMR (27 °C, CH_2Cl_2, 61.4 MHz): δ 1.59 (OD, bs, 1D), −9.76 (μ-D, s, 1D). $^{31}P\{^1H\}$ NMR (−80 °C; CD_2Cl_2, 161.9 MHz): δ 26.4 (Rh−P, ddm, 1P, $^2J_{trans\text{-}PP}$ = 312 Hz, $^1J_{RhP}$ = 105 Hz), 22.8 (Rh−P, ddm, 1P, $^2J_{trans\text{-}PP}$ = 312 Hz, $^1J_{RhP}$ = 105 Hz), −4.0 (Ir−P, dm, 1P, $^2J_{trans\text{-}PP}$ = 312 Hz), −6.9 (Ir−P, dm, 1P, $^2J_{trans\text{-}PP}$ = 312 Hz). ^{1}H NMR (−80 °C; CD_2Cl_2, 399.9 MHz): δ 6.10 (CH_2, m, 1H), 4.47 (CH_2, m, 1H), 4.01 (CH_2, m, 1H), 2.84 (CH_2, m, 1H), −9.93 (μ-H, ddm, 1H, $^1J_{RhH}$ = 17.6 Hz, $^2J_{HH}$ = 7.6 Hz); −12.27 (μ-H, ddm, 1H, $^1J_{RhH}$ = 20.6 Hz, $^2J_{HH}$ = 7.6 Hz).

*n. $[RhIr(CO)_2(Ge(OMe)Ph_2)(\mu\text{-}H)_2(dppm)_2][CF_3SO_3]$ (**16**).* To a septum-sealed Schlenk tube containing a solution of 70 mg (0.047 mmol) of $[RhIr(CO)_2(\mu\text{-}H)(\mu\text{-}GePh_2)(dppm)_2][CF_3SO_3]$ (**13**) in 2 mL of CH_2Cl_2 under argon was added 1.9 μL (0.047 mmol) of deoxygenated methanol. The dark green color of the solution changed to reddish orange within 5 min. After 30 min, addition of 5 mL of ether yielded an orange solid in 80% isolated yield. X-ray quality crystals were obtained by layering ether on a concentrated CH_2Cl_2 solution of **16** in an NMR tube. Anal. Calcd for $C_{66}H_{59}F_3GeIrO_6P_4RhS$: C, 51.87; H, 3.86. Found: C, 51.97; H, 3.93. The deuterium isotopologue of **16**, $[RhIr(CO)_2(Ge(OCD_3)Ph_2)(\mu\text{-}D)(\mu\text{-}H)(dppm)_2][CF_3SO_3]$ (**16-D$_4$**), was synthesized by reaction of **13** with 1 equiv of CD_3OD under similar conditions. $^{31}P\{^1H\}$ NMR (27 °C; CD_2Cl_2, 161.9 MHz): δ 24.5 (Rh−P, dm, 2P, $^1J_{RhP}$ = 104 Hz), −6.1 (Ir−P, m, 2P). ^{1}H NMR (27 °C; CD_2Cl_2, 498.1 MHz): δ 4.49 (CH_2, bm, 4H), 3.42 (OCH_3, s, 3H); −9.78 (μ-H, b, 1H), −12.16 (μ-H, b, 1H). ^{19}F NMR (27 °C; CD_2Cl_2, 376.3 MHz): δ 79.1 (CF_3SO_3, s, 3F). $^{31}P\{^1H\}$ NMR (−80 °C; CD_2Cl_2, 161.9 MHz): δ 24.9 (Rh−P, ddm, 1P, $^2J_{trans\text{-}PP}$ = 308 Hz, $^1J_{RhP}$ = 104 Hz), 22.8 (Rh−P, ddm, 1P, $^2J_{trans\text{-}PP}$ = 308 Hz, $^1J_{RhP}$ = 104 Hz), −5.8 (Ir−P, m, 2P). ^{1}H NMR (−80 °C; CD_2Cl_2, 399.9 MHz): δ 6.02 (CH_2, m, 1H), 4.57 (CH_2, m, 1H), 4.13 (CH_2, m, 1H), 2.47 (CH_2, m, 1H), −9.80 (μ-H, ddm, 1H, $^1J_{RhH}$ = 17.6 Hz, $^2J_{HH}$ = 7.1 Hz), −12.40 (μ-H, ddm, 1H, $^1J_{RhH}$ = 17.1 Hz, $^2J_{HH}$ = 7.6 Hz). $^{13}C\{^1H\}$ NMR (−80 °C, CD_2Cl_2, 125.7 MHz): δ 185.5 (Rh−CO, dt, 1C, $^1J_{RhC}$ = 77.0 Hz, $^2J_{PC}$ = 17.0 Hz), 175.7 (Ir−CO, t, 1C, $^2J_{PC}$ = 11.3 Hz), 36.3 (CH_2, m, 1C), 34.9 (CH_2, m, 1C).

*o. $[RhIr(CO)_2(GeClPh_2)(\mu\text{-}H)_2(dppm)_2][CF_3SO_3]$ (**17**).* To a septum-sealed Schlenk tube containing a solution of 85 mg (0.047 mmol) of $[RhIr(CO)_2(\mu\text{-}H)(\mu\text{-}GePh_2)(dppm)_2][CF_3SO_3]$ (**13**) in 2 mL of CH_2Cl_2 under argon was added 220 μL (0.26 mmol, 5 equiv) of a 2 M ether solution of HCl via a microliter syringe. The dark green solution immediately changed to reddish orange. Addition of 5 mL of ether resulted in a brick-red powder in 67% isolated yield. $^{31}P\{^1H\}$ NMR (27 °C; CD_2Cl_2, 161.9 MHz): δ 23.8 (Rh−P, dm, 1P, $^1J_{RhP}$ = 110 Hz), −7.3 (Ir−P, m). ^{1}H NMR (27 °C; CD_2Cl_2, 498.1 MHz): δ 4.48 (CH_2, bm, 2H), 4.26 (CH_2, bm, 2H), −10.27 (μ-H, b, 1H), −11.68 (μ-H, b, 1H). $^{13}C\{^1H\}$ NMR (27 °C, CD_2Cl_2, 125.7 MHz): δ 183.8 (Rh−CO, dt, 1C, $^1J_{RhC}$ = 75.0 Hz, $^2J_{PC}$ = 17.0 Hz), 174.6 (Ir−CO, t, 1C, $^2J_{PC}$ = 12.0 Hz). ^{19}F NMR (27 °C; CD_2Cl_2, 376.3 MHz): δ 79.1 (CF_3SO_3, s, 3F).

X-ray Data Collection and Structure Determination. *General Considerations.* Single crystals suitable for X-ray diffraction were obtained by slow diffusion of pentane into CH_2Cl_2 (**5**, **8**, **9**, **15**), benzene (**6**), fluorobenzene (**10**), or THF (**13**) solutions of the compounds or by diffusion of ether into THF (**14**) or dichloromethane (**16**) solutions of the compounds. Data were collected on either a Bruker D8/APEX II CCD diffractometer (**5**, **6**, **8**, **9**, **10**, **14**, **15**) or a Bruker PLATFORM/APEX II CCD (**13**, **16**) diffractometer at −100 °C using Mo Kα radiation.[20] Data were corrected for absorption through the use of Gaussian integration from indexing of the crystal faces. Structures were solved using the Patterson location of heavy atoms followed by structure expansion (*DIRDIF-2008*)[21] (**5**, **6**, **8**, **10**, **13**, **15**) or direct methods (*SHELXS-97*[22] (**9**, **16**), *SIR97*[23] (**14**)). Refinement was carried out using the program *SHELXL-97*.[22] Hydrogen atoms attached to carbons were assigned positions on the basis of the sp^2 or sp^3 hybridization geometries of their parent atoms and given isotropic displacement parameters 20% greater than the U_{eq}'s of their parent carbons. The hydroxyl hydrogen in **15** was generated in an idealized position (assuming sp^3 hybridization of the oxygen) with a displacement parameter 150% of that of the attached oxygen; the O−H bond vector was allowed to freely rotate with respect to the Ge−O bond during refinement. Metal hydrides for compound **5**, **6**, **9**, **13**, **14**, **15**, and **16** and Ge-bound hydrogens for **5**, **6**, **8**, and **14** were located from difference Fourier maps and treated as detailed below. A listing of crystallographic experimental data is provided for all structures as Supporting Information (Tables S1 and S2).

*Special Refinement Conditions. i. Compound **5**.* One metal atom position was refined with a site occupancy of 60% Ir/40% Rh (Ir(A)/Rh(B)); the other was refined as 60% Rh/40% Ir (Rh(A)/Ir(B)). The GeHPh and hydrido ligands were split into two sets of positions with relative occupancies of 80% (H(1A), H(2A), Ge(A), H(1GE), and the phenyl carbons C(91A) through C(96A)) and 20% (H(1B), H(2B), Ge(B), H(2GE), and the phenyl carbons C(91B) through C(96B)). Both metal−hydride (1.55 Å) and germyl−hydrogen (1.45 Å) distances were fixed during refinement.

*ii. Compound **6**.* One metal atom position was refined with a site occupancy of 60% Ir/40% Rh (Ir(A)/Rh(B)); the other was refined as 60% Rh/40% Ir (Rh(A)/Ir(B)). Both metal−hydride (1.55 Å) and germyl−hydrogen (1.45 Å) distances were fixed during refinement. Adjacent atomic positions for the disordered solvent dichloromethane molecule were refined with common isotropic displacement parameters.

*iii. Compound **8**.* Metal atom positions (designated Ir(A)/Rh(B) and Rh(A)/Ir(B)) were refined with a 50% site occupancy each of Ir and Rh. The coordinates and thermal parameter for the Ge-bound hydrogen (H1(GE)) were allowed to freely refine.

*iv. Compound **9**.* Metal atom positions (designated Ir(A)/Rh(B) and Rh(A)/Ir(B)) were refined with a 50% site occupancy each of Ir and Rh. The Ir(A)−H(1) and Rh(A)−H(2) distances were restrained to be 1.60(1) Å. Attempts to refine peaks of residual electron density as disordered or partial-occupancy solvent dichloromethane chlorine or carbon atoms were unsuccessful. Data were corrected for disordered solvent electron density through use of the SQUEEZE procedure as implemented in *PLATON*.[24] A total solvent-accessible void volume of 807 $Å^3$ with a total electron count of 282 (consistent with 6 molecules of solvent dichloromethane or 2 molecules per formula unit of the RhIr molecule) was found in the unit cell. The value of the Flack parameter observed herein (0.085(11)) was indicative of a minor degree of racemic twinning and accommodated during refinement (using the *SHELXL-97* TWIN instruction).

*v. Compound **10**.* The coordinates and thermal parameter for the hydrido ligand (H(1)) were allowed to freely refine, whereas the Ge(2)−H(2GE) distance (1.45 Å) was fixed during refinement. The F−C_{ipso} (1.35(1) Å) and F···C_{ortho} (2.37(1) Å) distances within the disordered solvent fluorobenzene molecules were restrained during refinement. One PhF molecule was split into two sets of positions with a 70%/30% distribution of occupancy factors; the aromatic rings of these molecules were modeled as idealized hexagons with a C−C bond distance of 1.39 Å and 120° bond angles.

*vi. Compound **13**.* One metal atom position was refined with a site occupancy of 55% Ir/45% Rh (Ir(A)/Rh(B)); the other was refined as 55% Rh/45% Ir (Rh(A)/Ir(B)). The coordinates and thermal parameter for the bridging hydrido ligand (H(1)) were allowed to freely refine. The O−C (1.45(1) Å) and C−C (1.50(1) Å) distances within the disordered solvent tetrahydrofuran molecules were restrained to idealized values during refinement.

*vii. Compound **14**.* The coordinates and thermal parameters for the hydrido ligands (H(1), H(2), H(3)) were allowed to freely refine. The O−C (1.45(1) Å) and C−C (1.50(1) Å) distances within the disordered solvent tetrahydrofuran molecule were restrained to idealized values during refinement. Attempts to refine peaks of residual electron density as additional disordered or partial-occupancy solvent tetrahydrofuran oxygen or carbon atoms were unsuccessful. Data were corrected for disordered solvent electron density through use of the SQUEEZE procedure as implemented in *PLATON*.[24] A total solvent-accessible void volume of 674 $Å^3$ with a total electron count of 167 (consistent with 4 molecules of solvent tetrahydrofuran or 2 molecules per formula unit of the Rh/Ir complex) was found in the unit cell.

*viii. Compound **15**.* Coordinates and thermal parameters for the bridging hydrido ligands (H(1), H(2)) were allowed to freely refine. Attempts to refine peaks of residual electron density as disordered or partial-occupancy solvent dichloromethane chlorine or carbon atoms were unsuccessful. Data were corrected for disordered solvent electron density through use of the SQUEEZE procedure as implemented in *PLATON*.[24] A total solvent-accessible void volume of 876.2 $Å^3$ with a total electron count of 264 (consistent with 6 molecules of solvent CH_2Cl_2 or 1.5 molecules of CH_2Cl_2 per formula unit of the Rh/Ir complex ion) was found in the unit cell.

*ix. Compound **16**.* Coordinates and thermal parameters for the bridging hydrido ligands (H(1), H(2)) were allowed to freely refine. The following distance restraints were applied to the partially occupied/disordered dichloromethane and diethyl ether molecules: C−Cl, 1.80(1) Å; C−C, 1.53(1) Å; C−O, 1.43(1) Å; C···C, 2.34(1) Å; C···O, 2.42(1) Å.

■ RESULTS AND CHARACTERIZATION OF COMPOUNDS

a. Reactions of [RhIr(CO)$_3$(dppm)$_2$] with Primary and Secondary Germanes. Reaction of [RhIr(CO)$_3$(dppm)$_2$] (**1**) with 1 equiv of phenylgermane at −80 °C in CD_2Cl_2 results in quantitative formation of the germyl/hydride complex [RhIr(H)(GeH$_2$Ph)(CO)$_2$(μ-CO)(dppm)$_2$] (**3**) by single Ge−H bond activation as shown in Scheme 1. The analogous complex, [RhIr(H)(GeH$_2$^{t}Bu)(CO)$_2$(μ-CO)(dppm)$_2$] (**4**), is also formed in the reaction of **1** with ^{t}BuGeH$_3$, although for this reaction a slightly elevated temperature (−40 °C) is required. The spectroscopic features of both compounds **3** and **4** are comparable (see experimental data); hence, only NMR data for compound **3** will be discussed. In these compounds, oxidative addition of the germane can occur at either Rh or Ir with migration of one of the fragments (either germyl or hydride) to the adjacent metal. Although Ir should have the greater tendency for oxidative addition, we view **1** as having a Rh(+1)/Ir(−1) formulation in which the saturated, pseudotetrahedral "Ir(CO)$_2$P$_2$$^-$" fragment functions as a 2-electron donor to Rh, giving the latter a square-planar 16e$^-$ configuration.[18] As a consequence of the unsaturation at Rh, we suggest that oxidative addition of the Ge−H bond occurs at this metal with hydride migration to Ir. This suggestion is also consistent with the presumed greater migratory tendency of the much smaller hydride than of the germyl ligand, since addition at Ir would necessitate migration of the germyl unit to Rh, in order to give the product observed (vide infra). The $^{31}P\{^1H\}$ NMR spectrum

Scheme 1

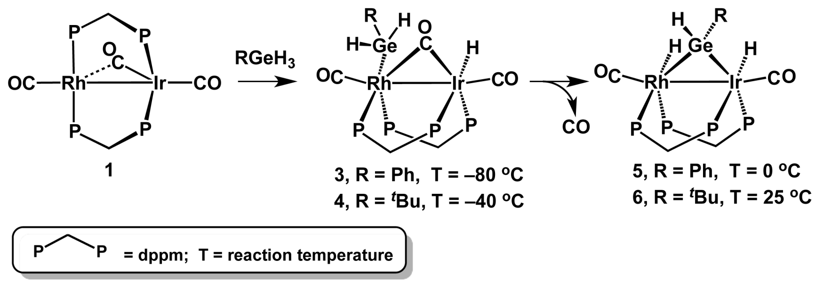

of **3** shows four well-resolved peaks at δ 37.5, 28.8, −5.5, and −12.4, indicating the chemical inequivalence of all ^{31}P nuclei; the two downfield resonances are attributed to the Rh-bound phosphorus nuclei, as indicated by the observed Rh−P coupling of 133 and 126 Hz. Of note, the $^{1}J_{Rh-P}$ value for the ^{31}P nucleus trans to the germyl ligand (126 Hz) is not much different from the value cis to the same ligand (133 Hz), suggesting that the germyl ligand does not exert a substantial trans influence. This is in contrast to the analogous silyl complex, in which the strong trans influence of the silyl ligand results in a substantially reduced $^{1}J_{Rh-P}$ value for the ^{31}P nucleus opposite this group.[15] In the ^{1}H NMR spectrum of **3** a doublet of doublets of doublets for the hydride resonance is observed at δ −11.50, displaying a large coupling of 125 Hz to the trans ^{31}P nucleus; the other couplings result from two other ^{31}P nuclei, as previously explained for the analogous silyl complexes.[15] The two diastereotopic Ge-bound hydrogens appear as two multiplets at δ 4.23 and 3.87. The positions of both germyl and hydride ligands, as shown in Scheme 1, were confirmed by selective ^{31}P decoupling and $^{13}C-^{1}H$ HMBC NMR experiments as previously described in the characterization of $[RhIr(H)(SiH_2Ph)(CO)_2(\mu\text{-}CO)(dppm)_2]$.[15] Three resonances at δ 178.0 (t), 198.2 (dt, $^{1}J_{Rh-C}$ = 78 Hz), and 229.9 ($^{1}J_{Rh-C}$ = 34 Hz) in the $^{13}C\{^{1}H\}$ NMR spectrum can be assigned to the Ir-bound, Rh-bound, and bridging CO ligands, respectively.

Warming the solution of **3** to 0 °C or reacting $[RhIr(CO)_3(dppm)_2]$ (**1**) with 1 equiv of phenylgermane at this temperature in CH_2Cl_2 leads to formation of the phenylgermylene-bridged dihydride, $[RhIr(H)_2(CO)_2(\mu\text{-}GeHPh)(dppm)_2]$ (**5**) (Scheme 1), the result of oxidative addition of two Ge−H bonds, one at each metal. The related *tert*-butylgermylene-bridged dihydride, $[RhIr(H)_2(CO)_2(\mu\text{-}GeH^tBu)(dppm)_2]$ (**6**), is obtained analogously. Both **5** and **6** exhibit very similar NMR spectra, except that complex **5** appears to be fluxional at room temperature (vide infra), while complex **6** shows no sign of fluxionality, having ^{31}P resonances that are sharp and well resolved between −80 °C and ambient temperature (see Supporting Information). At ambient temperature, compound **5** displays four broad unresolved resonances in the $^{31}P\{^{1}H\}$ NMR spectrum and at the same temperature the ^{1}H NMR spectrum shows three broad peaks at δ 5.42, 3.25, and 2.92 for the methylene protons (integrating as 2:1:1; the first resulting from coincidental overlap of two resonances) and two very broad peaks in the upfield region (δ −10.45 for Rh−H and −11.65 for Ir−H) for the metal-bound hydrides. Although the Ge-bound proton for **5** could not be located in the ^{1}H NMR spectrum, being obscured by the aromatic protons, the Ge−D resonance for $[RhIr(D)_2(CO)_2(\mu\text{-}GeDPh)(dppm)_2]$ (**5-D$_3$**) was observed at δ 6.92 in the ^{2}H NMR spectrum. For **6** the Ge−H resonance appears as a broad singlet at δ 6.70. Unfortunately, the IR data are of little use in further characterizing these species; in addition to the strong stretches for the terminal carbonyls in **5** and **6**, the only metal−hydride stretch for each compound is weak and broad at ca. 2090 cm^{-1} (as confirmed by deuterium labeling). However, the similarity of the NMR spectra with those of a silylene-bridged analogue[15] and the X-ray structures of **5** and **6** (vide infra) leave little doubt about their formulation. Upon cooling to −40 °C the $^{31}P\{^{1}H\}$ NMR resonances of **5** resolve into sharp multiplets at δ 27.1, 16.9, −10.0, and −14.0. The downfield pair of resonances are again assigned to the Rh-bound ^{31}P nuclei on the basis of their couplings (98 and 125 Hz) to ^{103}Rh. The substantially reduced Rh−P coupling of one of the Rh-bound ^{31}P nuclei is presumably a consequence of the greater trans influence of the hydride ligand than the bridging-germylene unit which is pseudotrans to the other Rh-bound ^{31}P nucleus (vide infra). The methylene protons and metal hydride peaks also become sharp and well resolved at this temperature, the latter of which display distinct coupling to the ^{31}P nucleus in the trans positions at each metal ($^{2}J_{HP}$ = 150 Hz; $^{2}J_{HP}$ = 127 Hz). A broad-band ^{31}P decoupling experiment also allows resolution of Rh coupling ($^{1}J_{RhH}$ = 12 Hz) in the former signal. The $^{13}C\{^{1}H\}$ NMR spectrum shows a doublet of multiplets at δ 193.8 ($^{1}J_{RhC}$ = 63 Hz) and a broad singlet at δ 180.3, attributed to Rh- and Ir-bound carbonyls, respectively.

Like its silylene-bridged counterpart, $[RhIr(H)_2(CO)_2(\mu\text{-}SiHPh)(dppm)_2]$,[15] the fluxionality of **5** appears to arise due to exchange between the three metal-bound hydrides. This exchange phenomenon was confirmed by saturation transfer NMR experiments at 0 °C, in which selective saturation of the Rh-bound hydride leads to collapse of the Ir-bound hydride and vice versa. We were unable to observe the effect of selective saturation on the Ge-bound hydrogen due to our inability to locate it in the NMR spectrum. This exchange process presumably occurs through rapid, reversible oxidative addition/reductive elimination involving the Ge−H bonds, as explained in our previous study on Si−H bond activation[15] and in related studies by Eisenberg and co-workers.[16] As noted earlier, complex **6** shows no sign of exchange at ambient temperature. In this case, the static nature of compound **6** can be attributed to the greater steric bulk of the *tert*-butyl group, which inhibits its fluxionality.

The structures of both complexes **5** and **6**, shown in Figure 1, highlight their similarities to each other and to their silylene analogues[15,17] in which the bridging-germylene ligand is pseudotrans to one diphosphine unit and the metal-bound hydrides are approximately trans to the other diphosphine unit (see Supporting Information for listing of bond lengths and angles). The distance between the two group 9 metals (2.8691(2) Å for **5** and 2.8736(2) Å for **6**)

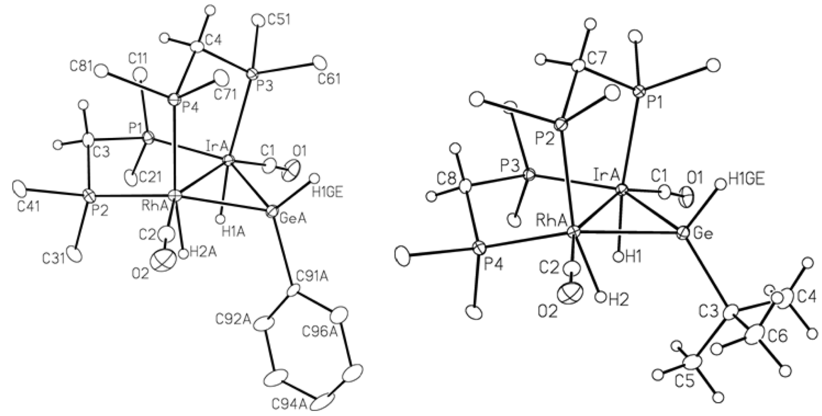

Figure 1. Perspective views of the major disordered form of compounds **5** (left) and **6** (right) showing the numbering scheme. Non-hydrogen atoms are represented by Gaussian ellipsoids at the 20% probability level. Hydrogen atoms are shown arbitrarily small. For the dppm phenyl groups, only the ipso carbons are shown. For **5**, Rh(A) and Ir(A) were refined at 60% occupancy while H(1A), H(2A), Ge(A), H(1GE), and the phenyl carbons C(91A)−C(96A) were refined at 80% occupancy. For **6**, Rh(A) and Ir(A) were refined at 60% occupancy.

suggests the presence of a formal metal−metal bond in each complex, while the Ir−Ge (Ir(A)−Ge(A) = 2.4234(4) Å for **5** and Ir−Ge = 2.4303(3) Å for **6**) and Rh−Ge distances (Rh(A)−Ge(A) = 2.4000(4) Å for **5** and Rh−Ge = 2.4294(3) for **6**) are symmetrical and slightly shorter than the previously reported homobimetallic Rh_2[5a] and Ir_2[5b] complexes. The Ir−Ge−Rh angles (73.00(1)° for **5** and 72.50(1)° for **6**) are also comparable to the values in the above homobimetallic systems[5] but larger than in one germylene-bridged diiridium complex for which the angle was more acute (Ir−Ge−Ir = 66.96(2)°).[2g] The metal-bound hydrides do not show a significant trans influence in the solid state as indicated by the closely comparable metal−phosphorus distances (ca. 2.34 Å for both structures; see Supporting Information) even though a substantially reduced Rh−P coupling constant was observed by $^{31}P\{^1H\}$ NMR spectroscopy for the Rh-bound ^{31}P nucleus which is trans to the hydride. Owing to the crystallographic disorder between the Rh and the Ir positions in these and some other compounds in this report, the X-ray studies cannot rule out the possibility of additional disorder involving Rh_2 and Ir_2 species. However, this possibility is unambiguously ruled out by the NMR studies, which show coupling of one end of the dppm ligands to ^{103}Rh, while the other end is Ir bound and displays no metal coupling.

Further reaction of **5** with 1 equiv of phenylgermane at room temperature leads to several unidentified products accompanied by H_2 evolution (as observed in the ^1H NMR). This, in contrast to the related silicon chemistry in which further reaction with phenylsilane, either in the presence or absence of CO, gave stable bis(silylene) complexes.[15] Even under an atmosphere of CO, reaction of **5** with another equivalent of phenylgermane again leads to a mixture of unidentified products.

However, reaction of **5** with phenylgermane at low temperature does give a single product. Addition of 1 equiv of $PhGeH_3$ to **5** at −80 °C results in no reaction, but upon warming to −40 °C a product is observed in the $^{31}P\{^1H\}$ NMR spectrum in about 30% yield after approximately 1 h reaction time (along with 70% unreacted **5**). This new species (**7**) displays four multiplets at δ 21.8, −10.5, −18.3, and −28.4 in the $^{31}P\{^1H\}$ NMR spectrum, the high-field resonance of which is close to that of free dppm (δ −23.0), suggesting that one arm of a diphosphine has dissociated and remains pendent. Only one resonance displays coupling to Rh ($^1J_{RhP}$ = 102 Hz), indicating that phosphine dissociation has taken place from the Rh end of one dppm group. Pendent dppm species have previously been observed in related silylene-bridged complexes of RhIr[15] and Rh_2[16] but interestingly were not observed in the less labile Ir_2[17] system. In the ^1H NMR spectrum two doublets of multiplets (at δ −12.10 for Rh−H ($^1J_{Rh-H}$ = 12 Hz) and −12.75 for Ir−H) and a broad resonance (at δ −12.58) are observed in a 1:1:1 ratio. The first two show distinct trans P−H coupling ($^2J_{P-H}$ = 159 and 129 Hz), indicating that one diphosphine unit maintains a trans disposition with respect to the metal hydrides. The last peak sharpens upon selective decoupling of each of the Ir- and Rh-bound ^{31}P nuclei, identifying it as bridging, and appears as a doublet ($^1J_{Rh-H}$ = 14 Hz) upon broad-band ^{31}P decoupling. The two diastereotopic Ge-bound hydrogens of the germyl group appear at δ 3.67 and 3.58 in the proton NMR. On the basis of these spectral data the product, $[RhIr(H)_2(GeH_2Ph)(CO)_2(\kappa^1\text{-dppm})(\mu\text{-H})(\mu\text{-GeHPh})(dppm)]$ (**7**) is assigned the structure shown. This species is unstable, and warming the reaction mixture to −20 °C leads to its transformation to several other unidentified products; nevertheless, it is clear that incorporation of a second germane into the original RhIrGe core is possible.

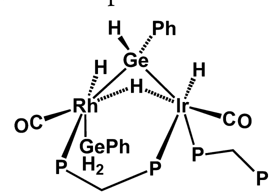

7

Although we were unable to generate a bis(phenylgermylene)-bridged species by reaction of **5** with phenylgermane, reaction of **5** with 1 equiv of diphenylgermane leads to an unprecedented mixed bis(germylene) complex $[RhIr(CO)_2(\mu\text{-GeHPh})(\mu\text{-GePh}_2)(dppm)_2]$ (**8**) in which both mono- and disubstituted germylene fragments are incorporated (Scheme 2). The $^{31}P\{^1H\}$ NMR spectrum of this complex shows four sharp, well-resolved resonances at δ 35.8, 24.4, 7.8, and −7.9 (again, the downfield pair of resonances show distinct Rh−P coupling), confirming the chemical inequivalence of all ^{31}P nuclei created by two different metals and different germylene bridges. Consistent with this formulation, the ^1H NMR spectrum displays four multiplets for the dppm methylene protons at δ 5.13, 4.49, 3.02, and 2.94 while the Ge-bound proton in the phenylgermylene unit appears as a

dx.doi.org/10.1021/ic2021269 | Inorg. Chem. 2012, 51, 4020−4034

Scheme 2

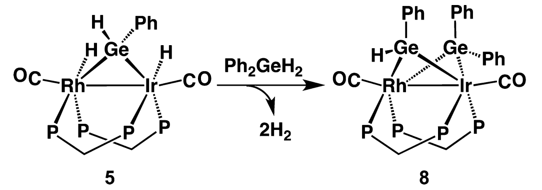

multiplet at δ 6.14. $^{13}C\{^{1}H\}$ NMR displays two resonances for Rh- and Ir-bound carbonyls at δ 200.5 and 187.0, respectively.

The solid-state structure of the bis(germylene) compound **8** is depicted in Figure 2, confirming incorporation of a second germylene unit. The Rh–Ir bond distance (2.8070(3) Å) is shorter than that for the monogermylene-bridged complexes (**5**, **6**, and **9** (vide infra)) where distances between 2.8691(2) and 2.8970(6) Å were observed, presumably resulting from incorporation of the second acutely bridging germylene unit. The Ir–Ge and Rh–Ge distances are comparable with those of the monogermylene-bridged complexes (see Supporting Information); however, the Rh–Ge–Ir angles (Ir(A)–Ge(1)–Rh(A) = 70.17(1)° and Ir(A)–Ge(2)–Rh(A) = 69.42(1)°) are more acute than the corresponding angles of compounds **5** (72.00(1)°), **6** (72.50(1)°), and **9** (72.42(3)°), consistent with the shorter Rh–Ir distance in **8**. The separation between the two bridging Ge atoms (Ge(1)–Ge(2) = 2.9921(6) Å) is significantly longer than a normal Ge–Ge bond (ca. 2.44 Å)[9a,b] but is also substantially shorter than the sum of their van der Waals radii (4.22 Å).[25] As a consequence, it is not clear whether this intermediate distance is a result of the steric demands within the complex or a weak interaction between these two metals.

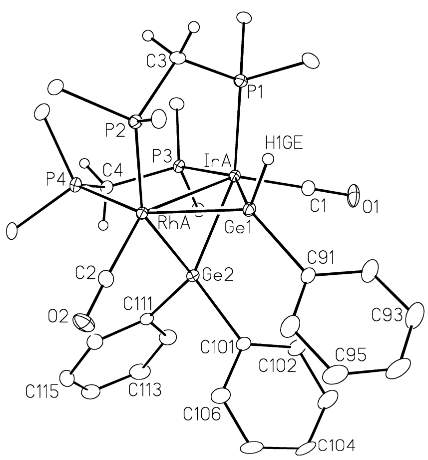

Figure 2. Perspective view of **8** showing the numbering scheme. Atom-labeling scheme and thermal parameters are as described in Figure 1. Rh(A) and Ir(A) were refined at 50% occupancy. For the dppm phenyl groups only the ipso carbons are shown.

Reaction of **1** with 1 equiv of diphenylgermane gives rise to the monogermylene-bridged complex, $[RhIr(H)_2(CO)_2(\mu\text{-}GePh_2)(dppm)_2]$ (**9**), in relatively low yield (40%) by double Ge–H bond activation (Scheme 3), as observed for the primary germanes. This species has very similar NMR features to complexes **5** and **6** and shows fluxional behavior at room temperature (as confirmed by variable-temperature NMR spectroscopy). Its structure is shown in Figure 3. Unlike the structures of **5** and **6**, which have the pair of hydride ligands on the same face of the Ir–Rh–Ge plane, the metal-bound hydrides in **9** occupy opposite faces of this plane. With the monosubstituted germylene groups (**5** and **6**) both small hydrides ligands are directed toward the bulkier germylene substituent (Ph or ^{t}Bu), allowing the bulky diphosphines to avoid these groups. However, in this disubstituted germylene group the symmetric environment on each side of the Ir–Rh–Ge plane favors one hydride on each side. As a consequence, there is significant twisting about the Rh–Ir bond (torsion angles P(1)–Ir–Rh–P(2) = 30.05(8)° and P(3)–Ir–Rh–P(4) = 29.92(8)°), allowing the dppm groups to minimize repulsions with the μ-$GePh_2$ group (for **5** these torsion angles are much smaller: P(1)–Ir–Rh–P(2) = 15.26(3)° and P(3)–Ir–Rh–P(4) = 13.86(3)°). The Rh–Ir distance (2.8790(6) Å) is again consistent with a formal metal–metal bond, while the Rh–Ge (2.437(1) Å) and Ir–Ge (2.437(1) Å) distances are closely comparable with those of complexes **5** and **6** (vide supra). The slight elongation of the Rh–P and Ir–P distances opposite the respective hydrides (2.346(2) and 2.335(2) Å) compared to those opposite the germylene unit (2.317(2) and 2.325(2) Å) may reflect the higher trans influence of the hydrides.

Scheme 3

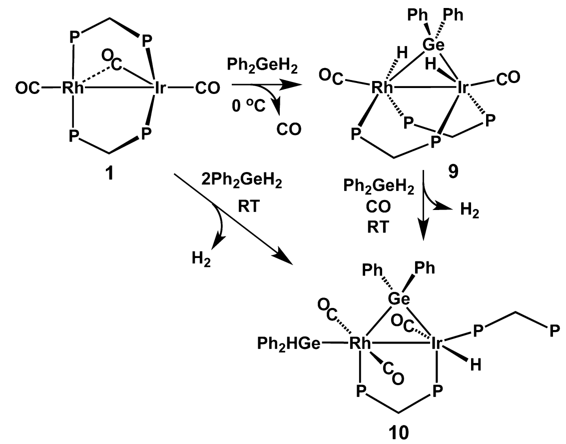

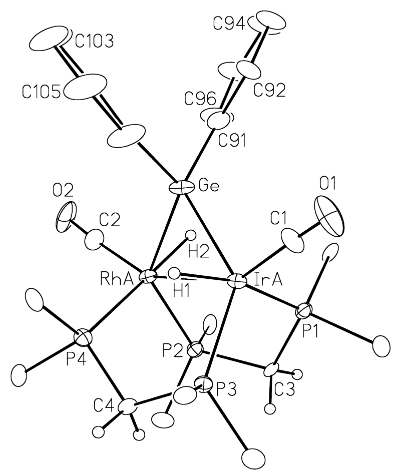

Figure 3. Perspective view of **9** showing the numbering scheme. Atom labeling scheme and thermal parameters are as described in Figure 1. Rh(A) and Ir(A) were refined at 50% occupancy. For the dppm phenyl groups only the ipso carbons are shown.

Reaction of **1** with 2 equiv of diphenylgermane in a sealed container or reaction of **9** with 1 equiv of diphenylgermane in the presence of 1 atm of CO leads to formation of the unusual germyl(germylene) complex, $[RhIr(H)(GeHPh_2)(CO)_3(\kappa^1\text{-dppm})(\mu\text{-GePh}_2)(dppm)]$ (**10**), accompanied by H_2 loss (see Scheme 3). Although the product yield under a CO atmosphere is quantitative, reaction of **1** without addition of CO is accompanied by decomposition, leading to low yields of **10** (according to $^{31}P\{^1H\}$ NMR). Reaction of **9** with diphenylgermane in the absence of CO leads only to decomposition. This behavior very much resembles that of the silylene-bridged analogue, $[RhIr(H)_2(CO)_2(\mu\text{-SiPh}_2)(dppm)_2]$,[15] and is in contrast to the reactivity of **1** with excess phenylgermane, which leads to decomposition at ambient temperature with or without CO.

The $^{31}P\{^1H\}$ NMR spectrum for compound **10** displays four resonances in a similar spin pattern as was observed for **7** with the upfield resonance (δ −28.5) representing the pendent end of one diphosphine. In the ^1H NMR spectrum of **10** the germyl hydrogen appears as a doublet at δ 5.65 ($^3J_{PH}$ = 6.1 Hz) and collapses to a singlet upon irradiation of the Rh-bound ^{31}P resonance, indicating that the germyl group is bound to Rh, although no resolvable coupling to Rh is observed. The Ir-bound hydride ligand appears as a doublet of doublets at δ −10.82 with approximately 15 and 20 Hz cis coupling to both Ir-bound ^{31}P nuclei as established by selective $^{31}P\{^1H\}$ decoupling experiments; the absence of Rh−H coupling indicates that this hydride is terminally bound to Ir. In the $^{13}C\{^1H\}$ NMR spectrum for **10** two Rh-bound carbonyl groups (δ 202.4 and δ 200.5, both displaying 43.8 Hz coupling to Rh) and one on Ir (δ 184.8) are observed.

An ORTEP drawing of **10** is shown in Figure 4, clearly confirming the germyl/germylene formulation and the pendent

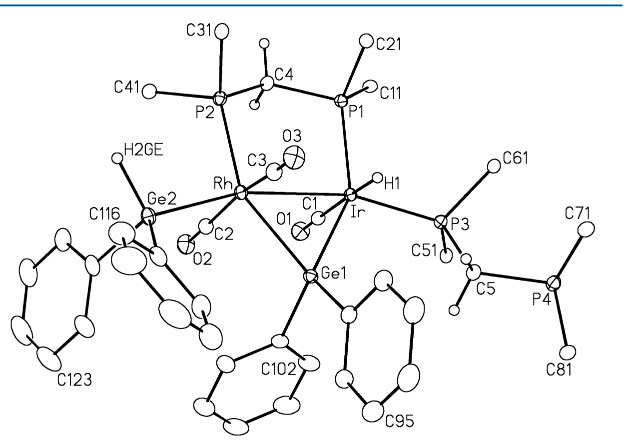

Figure 4. Perspective view of **10** showing the numbering scheme. Atom-labeling scheme and thermal parameters are as described in Figure 1. For the dppm phenyl groups only the ipso carbons are shown.

dppm arrangement. The Rh−Ge bond distances (Rh−Ge(1) = 2.4923(3) Å and Rh−Ge(2) = 2.4665(3) Å) are comparable to previously reported dirhodium germylene complexes;[8a] however, the Ir−Ge(1) distance (2.4103(2) Å) is slightly shorter than those previously reported.[2g,8b] The Ir-bound hydride was located and refined, lying trans to the Ir-bound CO with a typical Ir−H distance of 1.55(3) Å.

b. Reactions of $[RhIr(CH_3)(CO)_2(dppm)_2][CF_3SO_3]$ with Primary and Secondary Germanes. Reaction of cationic $[RhIr(CH_3)(CO)_2(dppm)_2][CF_3SO_3]$ (**2**) with 1 equiv of diphenylgermane at ambient temperature leads to a dark green, highly air- and moisture-sensitive, germylene- and hydride-bridged complex, $[RhIr(CO)_2(\mu\text{-GePh}_2)(\mu\text{-H})(dppm)_2][CF_3SO_3]$ (**13**), in high yield together with 1 equiv of methane (Scheme 4). The

Scheme 4

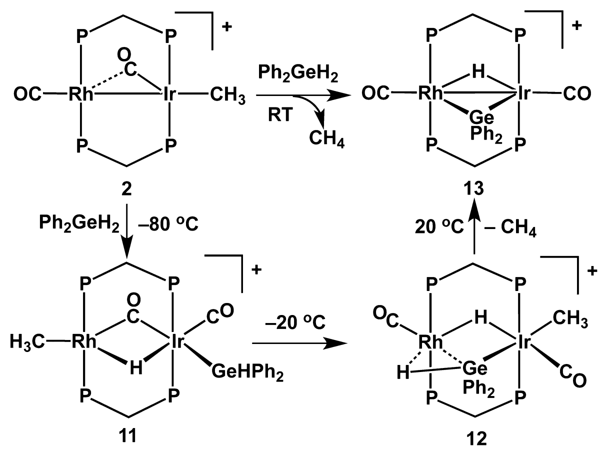

complex has been characterized by multinuclear NMR spectroscopy and X-ray structure determination.

Two resonances at δ 24.3 and 0.5 are observed in the $^{31}P\{^1H\}$ NMR spectrum of **13**, corresponding to the Rh- and Ir-bound ends of the diphosphines, and as is commonly observed, the downfield peak corresponds to that bound to Rh as confirmed by the large Rh−P coupling of 100 Hz. In the ^1H NMR spectrum a multiplet, corresponding to the bridging hydride ligand, appears at δ −9.91. Selective decoupling of each of the resonances for the Ir- and Rh-bound ^{31}P nuclei results in a collapse of the hydride resonance to a doublet of triplets, while ^{31}P broad-band decoupling gives a doublet ($^1J_{RhH}$ = 18.9 Hz). The $^{13}C\{^1H\}$ NMR spectrum displays a doublet of triplets for the Rh-bound CO ($^1J_{RhC}$ = 67.9 Hz, $^2J_{PC}$ = 14.0 Hz) and a triplet for the Ir-bound CO ($^2J_{PC}$ = 8.0 Hz). The complex shows no sign of fluxionality at room temperature, as both the $^{31}P\{^1H\}$ and the ^1H NMR spectra remain unchanged as the temperature is lowered to −80 °C.

X-ray structure determination of **13** (Figure 5) shows that unlike its neutral analogues (complexes **5**, **6**, and **9**), in which incorporation of a bridging germylene unit is accompanied by

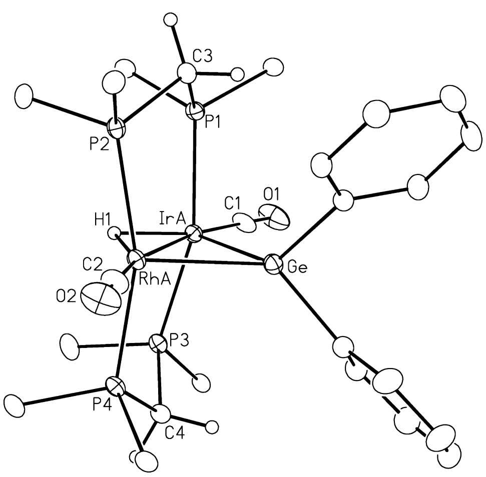

Figure 5. Perspective view of the complex cation of **13** showing the numbering scheme. Atom-labeling scheme and thermal parameters are as described in Figure 1. Rh(A) and Ir(A) were refined at 55% occupancy. For the dppm phenyl groups only the ipso carbons are shown.

bending back of the dppm units into a cradle-shaped geometry, the A-frame core of **13** is maintained, having an almost trans arrangement of diphosphines at each metal (P(1)−Ir(A)−P(3) = 160.90(4)° and P(2)−Rh(A)−P(4) = 162.19(3)°) with the bridging germylene unit on the face of the complex opposite the hydride ligand. The bending of the phosphines away from the μ-$GePh_2$ group and toward the much smaller hydride ligand allows the phenyl groups to minimize unfavorable contacts. The Rh−Ir bond length (2.8337(3) Å) of **13** is close to that of the starting complex **2** (2.8290(7) Å)[19] in spite of a bridging hydride ligand, which generally results in an increase in the associated metal−metal separation,[26] while the Ir−Ge and Rh−Ge distances in this cationic complex are found to be slightly elongated, and the Ir−Ge−Rh angle is more acute (69.11(1)°) than in the neutral analogue (vide supra). The disorder in the positions of the Rh and Ir atoms (a result of the symmetry of the complex) does not allow a differentiation of the bonds involving the group 9 metals; as a result, the bridging germylene and hydride groups appear to be symmetrically bridged (Rh(A)−Ge = 2.4875(5) Å, Ir(A)−Ge = 2.5088(5) Å and Rh(A)−H(1) = 1.77(4) Å, Ir(A)−H(1) = 1.75(4) Å).

When the reaction is monitored at low temperature two intermediates in the formation of **13** are observed by NMR spectroscopy (Scheme 4). Addition of 1 equiv of diphenylgermane to **2** at −80 °C gives rise to the first intermediate, a germyl/hydride complex, $[RhIr(CH_3)(GeHPh_2)(CO)(\mu\text{-H})(\mu\text{-CO})(dppm)_2][CF_3SO_3]$ (**11**), resulting from Ge−H bond activation at Ir accompanied by methyl migration from Ir to Rh. In complex **2** both metals are unsaturated, so the greater tendency for oxidative addition at the heavier congener favors addition to Ir. In the $^{31}P\{^1H\}$ NMR spectrum a doublet of multiplets appears at δ 28.3 ($^1J_{RhP}$ = 140 Hz) for the Rh-bound ^{31}P nuclei, while a multiplet at higher field (δ −9.1) appears for the Ir-bound ^{31}P nuclei. This pattern, characteristic of an AA′BB′X spin system, suggests an A-frame geometry for this intermediate. In the ^1H NMR spectrum, the germyl proton appears as a triplet at δ 5.09 and collapses to a singlet upon selective irradiation of the Ir-bound ^{31}P nuclei, while the bridging hydride appears as a doublet of multiplets at δ −8.94 and simplifies upon selective and broad-band ^{31}P decoupling (see Figure 6). The methyl protons appear as a triplet at δ 0.49 showing no apparent coupling to Rh; however, this resonance collapses to a singlet upon irradiation of the Rh-bound ^{31}P nuclei. The absence of resolvable two-bond Rh−H coupling in hydrocarbyl groups is common.[15,27] When $^{13}CH_3$-enriched complex **2** is used as starting material a doublet of triplets at δ 15.1 ($^1J_{RhC}$ = 28.0 Hz, $^2J_{PC}$ = 6.0 Hz) is observed in the $^{13}C\{^1H\}$ NMR spectrum for this methyl group, in which the magnitude of the coupling to Rh confirms its binding to this metal. The $^{13}C\{^1H\}$ NMR spectrum also displays two resonances at δ 214.8 and 173.3 assigned to the bridging and Ir-bound carbonyls, respectively. Upon broad-band phosphorus decoupling the terminally bound Ir−CO appears in the proton-coupled ^{13}C NMR spectrum as a doublet, displaying a trans C−H coupling of 26 Hz.

Upon warming to −20 °C the resonances in the $^{31}P\{^1H\}$ NMR spectrum due to **11** disappear completely, accompanied by the appearance of a new set corresponding to a second intermediate at δ 21.4 ($^1J_{Rh-P}$ = 99 Hz) and −15.6. This intermediate (Scheme 4) is formulated as $[RhIr(CH_3)(CO)_2(\mu\text{-H})(\mu\text{-GeHPh}_2)(dppm)_2][CF_3SO_3]$ (**12**), in which the Ge−H bond of the Ir-bound germyl ligand now interacts with Rh in an agostic fashion. In the ^1H NMR spectrum this

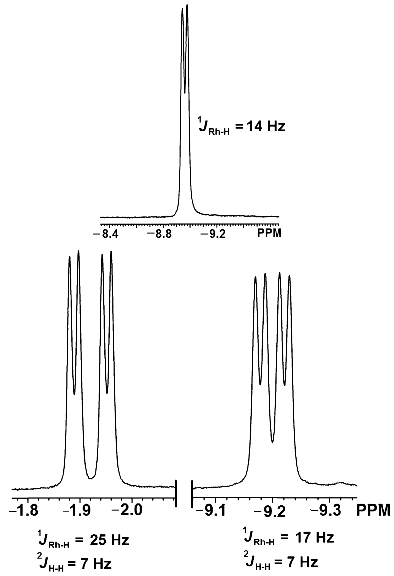

Figure 6. $^1H\{^{31}P\}$ NMR spectrum (broad-band ^{31}P decoupled) of high-field regions for complexes **11** (above) and **12** (below).

agostic hydride appears as a doublet of doublets of multiplets at δ −1.92 ($^1J_{Rh-H}$ = 25 Hz, $^2J_{H-H}$ = 7 Hz) showing coupling to Rh and two-bond coupling to the bridging hydride ligand (Figure 6). The upfield shift of this germyl-bridged proton compared to the terminal germyl protons in **3**, **4**, **7**, **10**, and **11** supports its agostic interaction. The bridging hydride at δ −9.23 displays coupling to Rh and to the agostic hydride ($^1J_{Rh-H}$ = 17 Hz, $^2J_{H-H}$ = 7 Hz), both of which are clear upon broad-band ^{31}P decoupling, shown in Figure 6, and both resonances sharpen upon selective decoupling of both Ir- and Rh-bound ^{31}P resonances indicating the involvement of these ligands with both metals. The ^1H NMR spectrum suggests migration of the methyl group back to Ir, as evidenced by its triplet resonance at δ 0.89 in the ^1H NMR which upon irradiation of the Ir-bound ^{31}P nuclei collapses to a singlet and by the triplet at ca. δ −25.1 ($^2J_{P-C}$ = 7.0 Hz) in the $^{13}C\{^1H\}$ NMR spectrum showing no Rh coupling. The high-field chemical shift of this signal is also consistent with an Ir-bound methyl ligand, in contrast to the Rh-bound methyl groups which tend to resonate significantly downfield as observed for **11**. The Rh-bound CO appears as a doublet of triplets at δ 192.4 ($^1J_{Rh-C}$ = 78.5 Hz), and the Ir-bound CO appears as a triplet at δ 177.5. In the proton-coupled ^{13}C NMR spectrum the latter resonance shows additional coupling ($^2J_{CH}$ = 26 Hz) due to the trans disposition of the bridging hydride. Upon warming to room temperature, reductive elimination of methane from Ir leads to exclusive formation of the hydride- and germylene-bridged complex **13**. We find it curious that methane elimination results at this stage and not earlier (from **11**) when the hydrides and methyl groups are adjacent on the more labile Rh center, although the failure for reductive elimination to occur from the lower oxidation state Rh is consistent with our Rh(I)/Ir(III) formulation for these species.

Reactions of complex **2** with 1 equiv of primary germanes (R = Ph or ^{t}Bu) under a variety of conditions do not occur cleanly but instead yield several unidentified complexes (according to NMR), so the reactions were not pursued further.

c. Reactivity of the Cationic Germylene-Bridged Complex (13). Attempts to synthesize a cationic germyl/germylene complex by reaction of $[RhIr(CO)_2(\mu\text{-GePh}_2)(\mu\text{-H})(dppm)_2]$

$[CF_3SO_3]$ (**13**) with an additional equivalent of diphenylgermane instead yields the germyl-bridged dihydride complex $[RhIr(H)(CO)_2(\mu\text{-}GeHPh_2)(\mu\text{-}H)(dppm)_2][CF_3SO_3]$ (**14**) (Scheme 5) as characterized by multinuclear NMR and X-ray diffraction analysis. Compound **14** is a rare example of a cationic germyl-bridged complex,[28] which is presumably formed by activation of a pair of Ge−H bonds in the added germane, followed by elimination of a "$GePh_2$" fragment, presumably as oligomers. An analogous silylene elimination was proposed to explain conversion of a monometallic Pt−silylene complex to a Pt−dihydride product.[29] Compound **14** can be viewed as the product of H_2 addition to **13**, and consistent with this interpretation, reaction of **13** with 1 atm of dihydrogen yields **14** within minutes (Scheme 5). Compound **14** can also be prepared from reaction of **13** with 1 equiv of diphenylsilane over a 6 h period with concomitant loss of a "$SiPh_2$" fragment. The fates of the germylene and silylene fragments produced in these reactions were not established.

Scheme 5

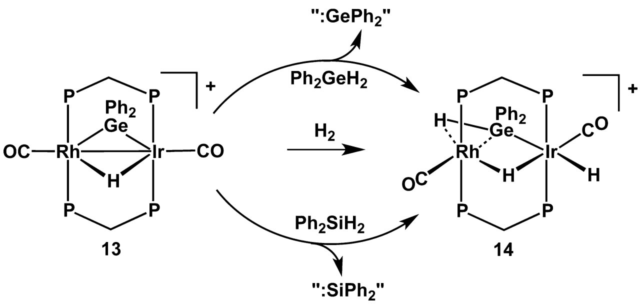

The ^1H NMR spectrum of **14** at 27 °C displays three broad peaks (barely above baseline) at δ −2.00, −9.62, and −10.30, which upon cooling to −78 °C sharpen while shifting to δ −2.77, −9.24, and −9.81 (see Supporting Information). The downfield peak is assigned to the agostic Ge−H unit on the basis of its chemical shift compared to classical metal hydrides. Upon ^{31}P broad-band decoupling this peak and the peak at δ −9.81 display coupling to Rh of 27.6 and 18.8 Hz, respectively. Selective ^{31}P decoupling of the Rh-bound ^{31}P resonance confirms that these two hydride signals also couple to these ^{31}P nuclei, while the resonance at δ −9.24 remains unchanged. However, upon selective ^{31}P decoupling of the Ir-bound ^{31}P nuclei, both high-field resonances sharpen, confirming the formulation in Scheme 5.

At intermediate temperatures a minor isomer of **14** (labeled as **14a**) is observed, so at −20 °C two new resonances are observed in the ^1H NMR spectrum at δ −10.6 and −11.3 in a 2:1 ratio and having approximately 10% of the total intensity of those due to **14**. This is accompanied by new broad $^{31}P\{^1H\}$ resonances at ca. δ 23.0 (almost buried under the corresponding resonance for **14**) and −6.8 (see Supporting Information). Clearly, the breadth of the ambient-temperature resonances for **14** is a result of exchange between these isomers, which is confirmed by saturation-transfer experiments at −20 °C. On the basis of the 2:1 integration ratio of hydride resonances of **14a**, we contemplated the possibility of dihydrogen/hydride species. However, this possibility was ruled out by the T_1 relaxation time measurements for the hydrides of both **14** and **14a** at −20 °C, in which all hydrides of both isomers have very similar relaxation times (ca. 0.4 s at 400 MHz). At lower temperatures the equilibrium between these isomers shifts in favor of **14** such that at −80 °C this is the only species visible in the NMR spectra. The breadth of the NMR resonances for **14a** and its low abundance over a relatively narrow temperature range did not allow us to further characterize this species.

The X-ray structure of the cation of complex **14** is shown in Figure 7. Again, the A-frame shape of the complex is maintained in the solid state, in which Rh adopts a trigonal bipyramidal arrangement (with the Ge−H bond occupying one site) while Ir is octahedral. The Rh−Ir distance is now elongated to 3.0273(2) Å from 2.8337(3) Å in the precursor (**13**), accompanied by a widening of the Rh−Ge−Ir angle, from 69.11(1)° to 72.253(8)° . This significant elongation of the Rh−Ir distance suggests the absence of a formal metal−metal bond in complex **14**. The Rh−Ge distance (2.6106(3) Å) is significantly longer than Ir−Ge (2.5228(3) Å), as expected for the agostic interaction involving Rh. This is supported by the Rh−H(3) bond distance of 1.85(3) Å, which is somewhat longer than expected for a classical hydride but clearly within the bonding distance. The bridging hydride (Rh−H(2) = 1.96(3) Å and Ir−H(2) = 1.67(3) Å) is found to be significantly more strongly bonded to Ir than to Rh possibly a result of the trans influence of the agostic Ge−H interaction. Surprisingly, this Rh−hydride interaction is even weaker than that of the agostic Ge−H interaction, consistent with the NMR results that showed a larger Rh coupling for the agostic hydride (vide supra). Both dppm groups are bent away from the bulky $GeHPh_2$ group toward the much smaller hydride ligand.

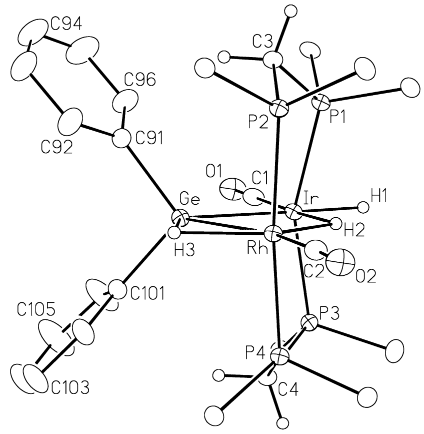

Figure 7. Perspective view of the complex cation of **14** showing the numbering scheme. Thermal parameters are as described in Figure 1. For the dppm phenyl groups only the ipso carbons are shown.

H_2 addition to **13** is reversible, so refluxing **14** in CH_2Cl_2 under an Ar flow regenerates the monohydride **13**. Reaction of **13** with D_2 initially yields the product (**14-D$_2$**) in which deuterium incorporation occurs as shown in Scheme 6. At 30 min after D_2 addition, ^2H NMR spectroscopy displays three high-field resonances at −78 °C analogous to the hydride resonances for **14** except that the highest field signal for the bridging group appears with very low intensity as a shoulder on the adjacent resonance. At same time, the ^1H resonance for **14-D$_2$** at −9.81 has changed little, integrating at approximately 0.8:2:2 with the pair of methylene proton resonances, while the two other resonances (at δ −2.77 and −9.24) appear with approximately one tenth of the intensity (see Supporting

Scheme 6

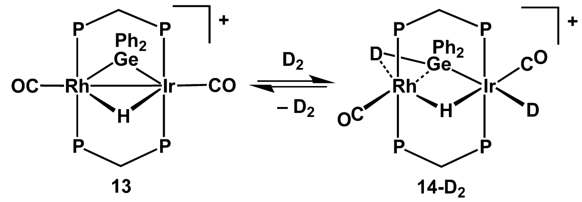

Information), indicating that initial deuterium incorporation is primarily on the germyl group and the Ir-bound hydride. Slight incorporation of deuterium in the bridging position suggests slow exchange involving all hydrides, and leaving the reaction mixture for 48 h leads to equal deuterium/hydrogen scrambling over all hydride positions, with all three of the hydride resonances at 1/3 of the intensity of a single hydrogen. A saturation transfer NMR experiment at −20 °C also indicates exchange between all the hydrides in which the selective saturation of any hydride signal leads to the significantly decreased intensity of the other two. In an attempt to understand how deuterium incorporation initially occurs in the two positions on *opposite sides* of the "$RhIrP_4$" plane, the reaction was monitored at low temperature but no intermediate was observed.

Compound **13** does not react with CO_2, in contrast to a monometallic platinum−germylene complex in which CO_2 reversibly couples to the metal−germylene unit.[6] However, this species reacts stoichiometrically with water, methanol, and HCl as shown in Scheme 7, leading to coordination of the

Scheme 7

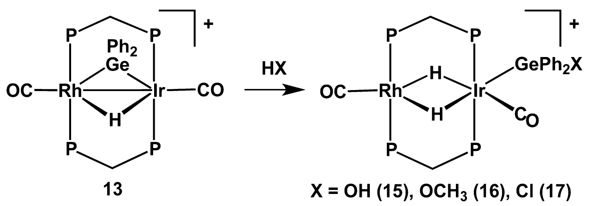

corresponding nucleophile at Ge and cleavage of the Rh−Ge bond yielding the germanol dihydride, $[RhIr(CO)_2(Ge(OH)Ph_2)(\mu\text{-}H)_2(dppm)_2][CF_3SO_3]$ (**15**), the germamethoxy dihydride, $[RhIr(CO)_2(Ge(OCH_3)Ph_2)(\mu\text{-}H)_2(dppm)_2][CF_3SO_3]$ (**16**), and the germylchloride dihydride, $[RhIr(CO)_2(GeClPh_2)(\mu\text{-}H)_2(dppm)_2][CF_3SO_3]$ (**17**), respectively. All have very comparable spectroscopic features. To our knowledge, the reactivity of water or methanol with either terminal or bridging germylene complexes has not previously been reported, although reaction of monometallic silylene and stannylene complexes with water is well documented.[29,30] Interestingly, the neutral germylene-bridged analogues (**5**, **6**, and **9**) do not react with water or methanol.

At ambient temperature the $^{31}P\{^1H\}$ NMR spectrum of **15** displays somewhat broad resonances: a doublet of multiplets at δ 24.4 for the Rh-bound ^{31}P nuclei and a multiplet at δ −5.7 for the Ir-bound ^{31}P nuclei. In the ^1H NMR spectrum a broad peak at δ 3.47 is observed for four methylene protons, a broad singlet at δ 1.41 corresponds to the hydroxyl group, and two broad multiplets at δ −9.81 and −12.05 appear for the bridging hydrides. The breadth of these resonances suggests fluxionality, and cooling a CD_2Cl_2 solution of **15** to −80 °C leads to four resonances in the $^{31}P\{^1H\}$ NMR spectrum at δ 26.4 (ddm, $^1J_{RhP}$ = 105 Hz, $^2J_{trans\text{-}PP}$ = 312 Hz), 22.8 (ddm), −4.0 (dm, $^2J_{trans\text{-}PP}$ = 312 Hz), and −6.9(dm). At this temperature the hydride resonances are sharper, showing coupling to Rh of 17.6 and 20.6 Hz, and upon broad-band decoupling of the ^{31}P nuclei, mutual coupling of 7.6 Hz between the hydrides is resolved. The $^{13}C\{^1H\}$ NMR displays a typical doublet of triplets and a triplet for Rh- and Ir-bound carbonyls. We assume that this fluxionality is a result of restricted rotation about the Ir−Ge bond, giving rise to top/bottom asymmetry in the static structure.

When the reaction of **13** is carried out with 1 equiv of D_2O, two resonances are observed at δ 1.59 and −9.76 in the ^2H NMR spectrum for the OD and bridging deuteride groups, respectively. However, unlike the observation for a monometallic Pd stannylene complex, water addition to **13** is not reversible;[29] surprisingly, no H/D exchange is observed when complex **15** is exposed to D_2O. Similarly, CH_3OH addition to **13** is not reversible as confirmed by CD_3OD addition to **16**.

The structures of both **15** and **16** have been confirmed by X-ray crystallography, and the ORTEP diagram of complex **16** is shown in Figure 8 (the structure of **15** is provided as

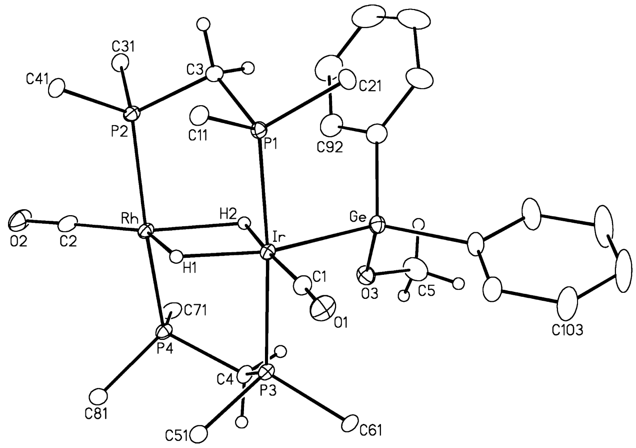

Figure 8. Perspective view of the complex cation of **16** showing the numbering scheme. Atom-labeling scheme and thermal parameters are as described in Figure 1. For the dppm phenyl groups only the ipso carbons are shown.

Supporting Information). The Rh−Ir distance in **16** (2.8605(3) Å) indicates a strong mutual attraction of the metals via the pair of bridging hydrides. These hydride ligands are significantly closer to Ir than to Rh (Rh−H(1) = 2.04(5) Å, Rh−H(2) = 1.89(4) Å), Ir−H(1) =1.67(5) Å, Ir−H(2) = 1.68(4) Å); nevertheless, the magnitude of the Rh−H coupling in the ^1H NMR spectrum is substantial for both ($^1J_{RhH}$ = 17.1 and 17.6 Hz).

■ DISCUSSION

In this study we investigated the formation of mixed-metal germyl and germylene complexes by Ge−H bond activation of primary and secondary germanes promoted by either of two complexes that involve the Rh/Ir metal combination. We had a number of goals in this study: (1) to discover what roles the two different metals might play in these activations; (2) to determine some mechanistic details about the stepwise activations; (3) to determine the differences in reactivity of

Scheme 8

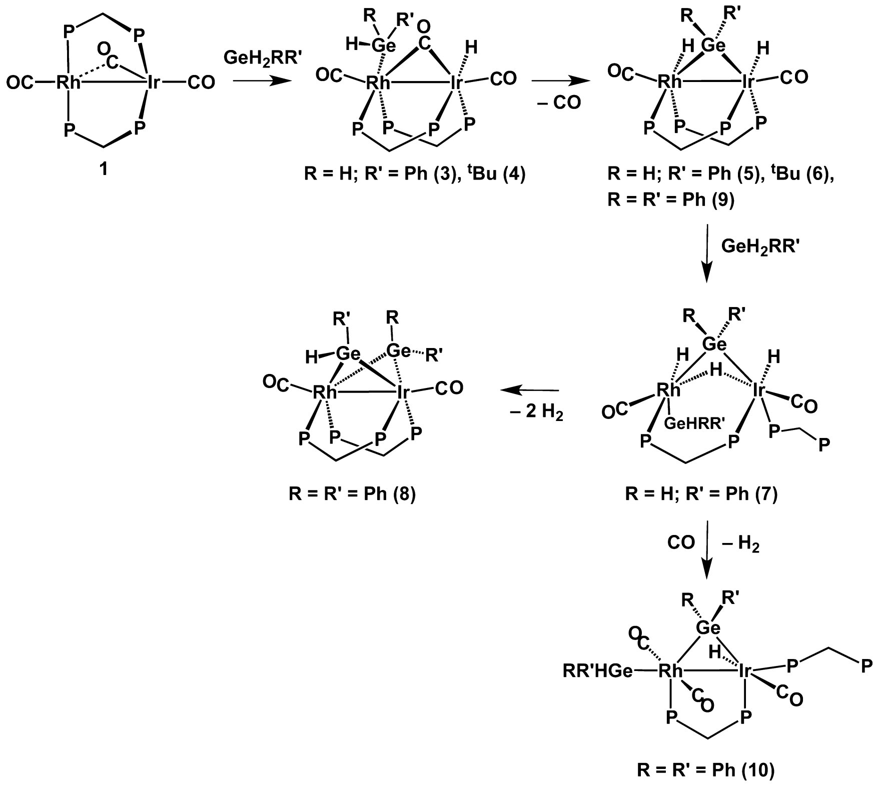

the two complexes (one neutral and other cationic); (4) to investigate the reactivity of bridging germylene groups; and (5) to compare the reactivities of silanes and less studied germane analogues. As will be explained, we have had some success in each of these goals.

The two complexes studied, $[RhIr(CO)_3(dppm)_2]$ (**1**) and $[RhIr(CH_3)(CO)_2(dppm)_2][CF_3SO_3]$ (**2**), although superficially similar, have some significant differences. Although compound **1**, being neutral and having only neutral ligands, appears to involve two metals in their zero oxidation state, we instead consider this species to be a mixed-valence Rh(+I)/Ir(−I) complex[18] in which the pseudotetrahedral "$Ir(CO)_2P_2^{-}$" moiety donates a pair of electrons to the "$Rh(CO)P_2^{+}$" center, giving Rh a square planar geometry. As such only Rh is coordinatively unsaturated. Compound **2** is related to **1** by formal replacement of CO by CH_3^+ and as such has two fewer electrons, having both metals unsaturated.

The above differences are initially seen in their low-temperature reactions with germanes during the first Ge−H bond activation step. Reaction with **1** occurs at the coordinatively unsaturated Rh center to yield a Rh-bound germyl ligand; even at −80 °C hydride migration to Ir has occurred. In contrast, the first step in the reaction of **2** with germanes occurs at Ir, yielding an Ir-bound germyl group, consistent with the greater tendency of this metal to undergo oxidative addition. Although the Ge−H bond activation steps presumably proceed through a σ complex involving the Ge−H bond being activated, such an intermediate is never seen. For the second Ge−H activation step, the germyl-bridged agostic intermediate is again not detected for reactions involving the neutral species **1**. However, agostically bridged germyl groups are observed in reactions involving the cationic species **2**; presumably the positive charge of **2** is enough to lower the tendency for activation of the second Ge−H bond, allowing such an intermediate to be observed.

In much of the chemistry investigated low-temperature studies allowed us to establish details about the stepwise activation processes involved and to determine the natures of some intermediates. To our knowledge, this is the only study to report such details about Ge−H bond activation. In the incorporation of up to two germanium-containing fragments by complex **1**, a number of intermediates were characterized at low temperature. As noted above, the first products of Ge−H bond activation, involving phenyl and *tert*-butylgermane, namely, $[RhIr(H)(GeH_2R)(CO)_2(\mu\text{-}CO)(dppm)_2]$ (R = Ph (**3**), ^{t}Bu (**4**)), were observed and characterized at −80 °C.

Incorporation of a second germanium-containing fragment in the germylene-bridged products has also been observed, although depending on the bridging germylene unit and the germane added several different (but related) outcomes are observed. Surprisingly, incorporation of a second equivalent of phenylgermane into the phenylgermylene-bridged product $[RhIr(H)_2(CO)_2(\mu\text{-}GeHPh)(dppm)_2]$ (**5**) is only observed at low temperature with decomposition occurring when this product is warmed above −40 °C. This low-temperature intermediate, $[RhIr(H)_2(GeH_2Ph)(CO)_2(\kappa^1\text{-}dppm)(\mu\text{-}H)(\mu\text{-}GeHPh)(dppm)]$ (**7**), is the result of dissociation of the Rh end of one bridging dppm group accompanied by oxidative addition of phenylgermane at the unsaturated Rh center.

In contrast, reaction of **5** with diphenylgermane (Scheme 2) yields the mixed digermylene-bridged product $[RhIr(CO)_2(\mu\text{-}GeHPh)(\mu\text{-}GePh_2)(dppm)_2]$ (**8**) with the elimination of 2 equiv of H_2. Although these are dramatically different results, they are in fact closely related as proposed in Scheme 8, which depicts the different species observed in the reactivity of **1** with different germanes and the possible relationships between them. We assume that reaction of **5** with diphenylgermane proceeds via an intermediate analogous to **7** and that subsequent transformation to **8** occurs by a sequence of steps involving H_2 elimination, oxidative addition of the remaining Ge−H bond of the germyl group, elimination of the second equivalent of H_2, and recoordination of the pendent end of the κ^1-diphosphine at Rh. It is not clear why an analogous species containing two bridging phenylgermylene groups was not obtained in the reaction of **5** with phenylgermane, but presumably the additional germanium-bound hydrogen, which would be prone to oxidative addition, and the smaller size of the monosubstituted germyl ligand in **7**, which allows more facile approach to the adjacent metal, play a role.

The third variation in reactivity with a second germane is seen in the reaction of $[RhIr(H)_2(CO)_2(\mu\text{-}GePh_2)(dppm)_2]$ (**9**) with diphenylgermane (Schemes 3 and 8) which results in decomposition in the absence of CO but yields $[RhIr(H)(GeHPh_2)(CO)_3(\kappa^1\text{-dppm})(\mu\text{-}GePh_2)(dppm)]$ (**10**) under a CO atmosphere. This product is closely related to **7** (apart from the different substituents on Ge), in which two hydride ligands have been replaced by CO. We assume that when the initial trihydride, diphenylgermyl intermediate, analogous to **7**, loses H_2, oxidative addition of the germyl−H bond to give a bis-diphenylgermylene-bridged product analogous to **8** is inhibited, owing to the greater bulk of the disubstituted germyl and germylene groups. Since the pendent dppm is also too bulky to recoordinate, decomposition occurs in the absence of an additional ligand required to alleviate the unsaturation. However, under CO the stable tricarbonyl species **10** is formed, having both metals coordinatively saturated. The coordinative unsaturation required for reaction of the saturated species $[RhIr(H)_2(CO)_2(\mu\text{-}GeRR')(dppm)_2]$ with a second equivalent of germane can result either from dissociation of the Rh end of a diphosphine (two examples of compounds containing a pendent dppm group were characterized), or from reductive elimination of a hydride and a germylene fragment from one metal to give an unsaturated germyl compound, since exchange of the germylene hydrogen with the Rh- and Ir-bound hydrides is proposed to occur by such a process.

In spite of the current interest in late transition-metal catalysts containing germanium in hydrogenation reactions, surprisingly little has been published on the reactivity of mixed transition-metal/germanium-containing complexes with H_2; in fact, the reactivity of germyl and germylene-bridged complexes has to date received very little attention. In this paper we report the addition of H_2 and HX (X = OH, OMe, Cl) to a cationic germylene-bridged Rh/Ir complex. Although mechanistically these two reaction types (with H_2 or HX) presumably differ, the final products have some similarities. In both cases the transfer of one hydrogen to the transition metals occurs while either H or X binds to Ge, converting the μ-germylene to a germyl ligand. In the H_2 reaction the diphenylgermyl ligand produced is bridging, interacting with Rh in an agostic manner via a Ge−H bond, while the polar substrates all yield terminal germyl groups. The extremely facile migration of a hydrogen from one face of the "$RhIrP_4$" plane to the other upon reaction of **13** with H_2 (even at −40 °C) suggests a deprotonation/reprotonation step rather than the concerted rearrangement of ligands, although the counteranion used (BPh_4^-, $BAr^F{}_4^-$ or OTf^-) plays no obvious role in such a transfer, with no rate difference being observed with these counteranions.

Finally, as suggested in the Introduction and alluded to throughout this paper, the chemistry of compounds **1** and **2** with germanes displays many similarities to that involving the analogous silanes. However, some subtle differences are observed. Our inability to generate complexes containing two bridging monosubstituted germylene groups is in contrast to the related silylene species, which are readily obtained, and suggests a more facile oxidative addition of the remaining Ge−H bond of the targeted μ-GeHR unit compared to Si−H, consistent with the weaker Ge−H than Si−H bonds. Exclusive formation of the germylene- and hydride-bridged complex $[RhIr(CO)_2(\mu\text{-}GePh_2)(\mu\text{-}H)(dppm)_2][CF_3SO_3]$ (**13**) from reaction of **2** with diphenylgermane is another subtle difference from the silane chemistry in which reaction of **2** with 1 equiv of diphenylsilane led to the two different products: a silylene/hydride-bridged complex, $[RhIr(CO)_2(\mu\text{-}SiPh_2)(\mu\text{-}H)(dppm)_2][CF_3SO_3]$ (analogous to **13**), and a silylene-bridged, acetyl complex, $[RhIr(CO)_2(H)(C(CH_3)O)(\mu\text{-}H)(\mu\text{-}SiPh_2)(dppm)_2][CF_3SO_3]$ (formed by methyl migration to a carbonyl ligand in competition to methane loss from the precursor).[15] This latter result demonstrates the greater trans-labilizing effect of the silyl group,[31] which promotes migration of the methyl ligand in an intermediate such as **12** to the adjacent carbonyl.

■ ASSOCIATED CONTENT

Supporting Information

Tables of crystallographic experimental details and selected bond distances and angles for compounds **5**·C_6H_6, **6**·CH_2Cl_2, **8**·CH_2Cl_2, **9**·$2CH_2Cl_2$, **10**·$1.5C_6H_5F$, **13**·$3C_4H_8O$, **14**·$4C_4H_8O$, **15**·$2CH_2Cl_2$, and **16**·$1.5CH_2Cl_2$·$0.5C_4H_8O$; selected NMR spectra for compounds **5**, **6**, **8**, **10**, **13**, and **14** in pdf format; atomic coordinates, interatomic distances and angles, anisotropic thermal parameters, and hydrogen parameters for these compounds in CIF format. This material is available free of charge via the Internet at http://pubs.acs.org.

■ AUTHOR INFORMATION

Corresponding Author

*Phone: 017804925581. Fax: 017804928231. E-mail: martin.cowie@ualberta.ca.

Notes

The authors declare no competing financial interest.

■ ACKNOWLEDGMENTS

We thank the Natural Sciences and Engineering Research Council of Canada (NSERC) and the University of Alberta for providing financial support for this research. We thank NSERC for funding the Bruker D8/APEX II CCD diffractometer and Nicolet Avatar FTIR spectrometer. M.H.M. thanks the Bangladesh Council of Scientific and Industrial Research (BCSIR) for granting him a study leave at the University of Alberta and the Government of Alberta for funding support (Q.E. II Scholarship). We thank the Department's Analytical and Instrumentation Laboratory and NMR facility for their outstanding support.

■ REFERENCES

(1) (a) Shinohara, A.; McBee, J.; Tilley, T. D. *Inorg. Chem.* **2009**, *48*, 8081. (b) Hayes, P. G.; Waterman, R.; Glaser, P. B.; Tilley, T. D. *Organometallics* **2009**, *28*, 5082. (c) Takaoka, A.; Mendiratta, A.; Peters, J. C. *Organometallics* **2009**, *28*, 3744. (d) Feldman, J. D.; Peters, J. C.; Tilley, T. D. *Organometallics* **2002**, *21*, 4065.

(2) (a) Tanabe, M; Ishikawa, N.; Osakada, K. *Organometallics* **2006**, *25*, 796. (b) Usui, Y.; Hosotani, S.; Ogawa, A.; Nanjo, M.; Mochida, K. *Organometallics* **2005**, *24*, 4337. (d) White, C. P.; Braddock-Wilking, J.; Corey, J. Y.; Xu, H.; Redekop, E.; Sedinkin, S.; Rath, N. P.

Organometallics **2007**, *26*, 1996. (e) Arii, H.; Nanjo, M.; Mochida, K. *Organometallics* **2008**, *27*, 4147. (f) Mohamed, B. A. S.; Kikuchi, M.; Ueno, K.; Tobita, H.; Ogino, H. *Chem. Lett.* **2004**, *33*, 112. (g) Hawkins, S. M.; Hitchcock, P. B.; Lappert, M. F.; Rai, A. K *J. Chem. Soc., Chem. Commun.* **1986**, *18*, 1689.

(3) (a) Bodnar, Z.; Mallat, T.; Bakos, I.; Szabo, S.; Zsoldos, Z.; Schay, Z. *Appl. Catal., A* **1993**, *102*, 105. (b) Lafaye, G.; Micheaud-Especel, C.; Montassier, C.; Marcot, P. *Appl. Catal. A: Gen.* **2004**, *257*, 107. (c) Lafaye, G.; Micheaud-Especel, C.; Montassier, C.; Marcot, P. *Appl. Catal. A: Gen.* **2002**, *230*, 19. (d) Ekou., T.; Vicente, A.; Lafaye, G.; Especel, C.; Marcot, P. *Appl. Catal. A: Gen.* **2006**, *314*, 73.

(4) (a) Macleod, N.; Freyer, J. R.; Stirling, G.; Webb, G. *Catal. Today* **1998**, *46*, 37.

(5) (a) Adams, R. D.; Trufan, E. *Inorg. Chem.* **2010**, *49*, 3029. (b) Adams, R. D.; Trufan, E. *Organometallics* **2010**, *29*, 4346. (c) Adams, R. D.; Trufan, E. *Inorg. Chem.* **2009**, *48*, 6124. (d) Adams, R. D.; Captain, B.; Trufan, E. *J. Cluster Sci.* **2007**, *18*, 642.

(6) Litz, K. E.; Henderson, K.; Gourley, R. W.; Holl, M. M. B. *Organometallics* **1995**, *14*, 5008.

(7) Litz, K. E.; Kempf, J. W.; Holl, M. M. B. *J. Am. Chem. Soc.* **1998**, *120*, 7484.

(8) (a) Cygan, Z. T.; Bender, J. E. IV; Litz, K. E.; Kempf, J. W.; Holl, M. M. B. *Organometallics* **2002**, *21*, 5373. (b) York, J. T.; Young, V. G. Jr.; Tolman, W. B. *Inorg. Chem.* **2006**, *45*, 4191.

(9) (a) Tanabe, M.; Ishikawa, N.; Hanzawa, M.; Osakada, K. *Organometallics* **2008**, *27*, 5152. (b) Tanabe, M.; Hanzawa, M.; Ishikawa, N.; Osakada, K. *Organometallics* **2009**, *28*, 6014. (c) Tanabe, M.; Osakada, K. *Organometallics* **2010**, *29*, 4702.

(10) (a) Corey, J. Y.; Braddock-Wilking, J. *Chem. Rev.* **1999**, *99*, 175 and references therein. (b) Corey, J. Y. *Chem. Rev.* **2011**, *111*, 863 and references therein.

(11) (a) Waterman, R.; Hayes, P. G.; Tilley, T. D. *Acc. Chem. Res.* **2007**, *40*, 712. (b) Okazaki, M.; Tobita, H.; Ogino, H. *Dalton Trans.* **2003**, 493.

(12) (a) Marciniec, B. *Silicon Chem.* **2002**, *1*, 155. (b) Brook, M. A. *Silicon in Organic, Organometallic, and Polymer Chemistry*; Wiley: New York, 2000. (c) Calimano, E.; Tilley, T. D. *J. Am. Chem. Soc.* **2009**, *131*, 11161. (d) Ojima, I.; Kogure, T.; Nihonyanagi, M.; Nagai, Y. *J. Chem. Soc., Chem. Commun.* **1972**, 938. (e) Ojima, I.; Nihonyanagi, M.; Nagai, Y. *Bull. Chem. Soc. Jpn.* **1972**, *45*, 3506. (f) Jiménez, M. V.; Pérez-Torrente, J. J.; Bartolomé, M. I.; Gierz, V.; Lahoz, F. J.; Oro, L. A. *Organometallics* **2008**, *27*, 224.

(13) (a) Aitken, C. T.; Harrod, J. F.; Samuel, E. *J. Am. Chem. Soc.* **1986**, *108*, 4059. (b) Tilley, T. D. *Acc. Chem. Res.* **1993**, *26*, 22. (c) Rosenberg, L.; Davis, C. W.; Yao, J. Z. *J. Am. Chem. Soc.* **2001**, *123*, 5120. (d) Fontaine, F.-G.; Zargarian, D. *J. Am. Chem. Soc.* **2004**, *126*, 8786.

(14) (a) Luo, X. L.; Crabtree, R. H. *J. Am. Chem. Soc.* **1989**, *111*, 2527. (b) Biffis, A.; Basato, M.; Brichese, M.; Ronconi, L.; Tubaro, C.; Zanella, A.; Graiff, A; Tiripicchio, A. *Adv. Synth. Catal.* **2007**, 2485.

(15) Mobarok, M. H.; Oke, O.; Ferguson, M. J.; McDonald, R.; Cowie, M. *Inorg. Chem.* **2010**, *49*, 11556.

(16) (a) Wang, W.-D.; Hommeltoft, S. I.; Eisenberg, R. *Organometallics* **1988**, *7*, 2417. (b) Wang, W.-D.; Eisenberg, R. *J. Am. Chem. Soc.* **1990**, *112*, 1833. (c) Wang, W.-D.; Eisenberg, R. *Organometallics* **1991**, *10*, 2222. (d) Wang, W.-D.; Eisenberg, R. *Organometallics* **1992**, *11*, 908.

(17) McDonald, R.; Cowie, M. *Organometallics* **1990**, *9*, 2468.

(18) McDonald, R.; Cowie, M. *Inorg. Chem.* **1990**, *29*, 1564.

(19) Oke, O.; McDonald, R.; Cowie, M. *Organometallics* **1999**, *18*, 1629.

(20) Programs for diffractometer operation, data collection, data reduction, and absorption correction were those supplied by Bruker

(21) Beurskens, P. T.; Beurskens, G.; de Gelder, R.; Smits, J. M. M.; Garcia-Granda, S.; Gould, R. O. *The DIRDIF-2008 program system*; Crystallography Laboratory, Radboud University Nijmegen: The Netherlands, 2008.

(22) Sheldrick, G. M. *Acta Crystallogr.* **2008**, *A64*, 112−122.

(23) Altomare, A.; Burla, M. C.; Camalli, M.; Cascarano, G. L.; Giacovazzo, C.; Guagliardi, A.; Moliterni, A. G. G.; Polidori, G.; Spagna, R. *J. Appl. Crystallogr.* **1999**, *32*, 115−119.

(24) (a) Sluis, P.; van der; Spek, A. L. *Acta Crystallogr.* **1990**, *A46*, 194−201. (b) Spek, A. L. *Acta Crystallogr.* **1990**, *A46*, C34. (c) Spek, A. L. *J. Appl. Crystallogr.* **2003**, *36*, 7−13.

(25) Mantina, M.; Chamberlin, A. C.; Valero, R.; Cramer, C. J.; Truhlar, D. G. *J. Phys. Chem. A* **2009**, *113*, 5806.

(26) Bau, R.; Drabnis, M. H. *Inorg. Chim. Acta* **1997**, *259*, 27.

(27) Trepanier, S. J.; Dennett, J. N. L.; Sterenberg, B. T.; McDonald, R.; Cowie, M. *J. Am. Chem. Soc.* **2004**, *126*, 8046.

(28) Ogino, H.; Tobita, H. *Adv. Organomet. Chem.* **1998**, *42*, 223.

(29) Feldman, J. D.; Mitchell, G. P.; Nolte, J.-O.; Tilley, T. D. *J. Am. Chem. Soc.* **1998**, *120*, 11184.

(30) (a) Hayes, P. G.; Gribble, C. W.; Waterman, R.; Tilley, T. D. *J. Am. Chem. Soc.* **2009**, *131*, 4606. (b) Schager, F.; Seevogel, K.; Pörschke, K. R.; Kessler, M.; Krüger, C. *J. Am. Chem. Soc.* **1996**, *118*, 13075.

(31) (a) Minato, M.; Zhou, D.-Y.; Sumiura, K.; Hirabayashi, R.; Yamaguchi, Y.; Ito, T. *Chem. Commun.* **2001**, 2654. (b) Minato, M.; Nishiuchi, J.-Y.; Kakeya, M.; Matsumoto, T.; Yamaguchi, Y.; Ito, T. . *Dalton Trans.* **2003**, 483.